e-HIGHWAY 2050

Modular Development Plan of the Pan-European Transmission System 2050

Contract number	308908	**Instrument**	Collaborative Project
Start date	1st of September 2012	**Duration**	40 months
WP 8	**Enhanced Pan-European Transmission Planning Methodology**		
D8.3a	**Enhanced methodology to define optimal grid architectures for 2050**		

		Date & Visa
Written by	Sara Lumbreras, Fernando Banez-Chicharro, COMILLAS Camille Pache, RTE	19/06/2015
Checked by	Peter Van Roy, ELIA Alexander Weber, TU BERLIN Patrick Panciatici, Camille Pache, Jean Maeght, RTE	24/06/2015
Validated by	Nathalie Grisey, Gérald Sanchis, RTE	27/07/2015

Project co-funded by the European Commission within the Seventh Framework Programme		
Dissemination Level		
PU	Public	X
PP	Restricted to other programme participants (including the Commission Services)	
RE	Restricted to a group specified by the consortium (including the Commission Services)	
CO	Confidential, only for members of the consortium (including the Commission Services)	

Document information

General purpose

This document is the deliverable D8.3.a of the e-Highway2050 project. It contains the description of the work performed in the framework of Task 8.3, named “Detection of system overloads and transmission planning for 2050”.

This deliverable:

- describes the method which has been developed and prototyped in the framework of this work package,
- discusses the modelling choices which have been made in the context of this long-term pan-European study and under the light of the state-of-the-art,
- and illustrates the methodology through test-cases and examples.

Change status

Revision	Date	Changes description	Authors
V1.0	30.04.2015	Initial version	S. Lumbreras F. Banez-Chicharro C. Pache
V1.1	19.06.2015	Modifications after exchanges within WP8	F. Banez-Chicharro
V1.2	03.07.2015	Modifications after review by the quality pool	C. Pache
V1.3	27.07.2015	Modifications after review by project partners	C. Pache

EXECUTIVE SUMMARY

Even though there has been a long array of literature applied to Transmission Expansion Planning (TEP), the complexities inherent to the problem mean that large-scale, long-term TEP still remains a challenge. As a result, most practical TEP implementations are based on expert judgement. The aim of WP8 within project e-Highway2050 is to propose a suitable methodology that exploits the techniques that have been developed in the literature and extends them further in order to tackle a system as large as the European one.

We propose a methodology that is based on a combination of simulation and optimization. Simulation tries to represent the possible states of the system in as much detail as required. The perspective taken is that of a Transmission System Operator (TSO) which undertakes centralized TEP with no control over generation expansion, which is taken into account under the form of uncertain generation scenarios, so that several possible evolutions of the power sector are considered. Other sources of uncertainty, such as demand or non-controllable generation are also taken into account in the simulation. This incorporates spatial and time correlation effects, so that the full set of hourly time series generated can be considered sufficiently representative of the behaviour of the system.

These simulated results are too detailed both in number of nodes and number of operation snapshots to be subject to optimization directly. Therefore, we apply reduction methods to condense the information into a workable model: snapshot selection techniques single out the most representative operation situations and network reduction mechanisms condense the full grid into a smaller network that still maintains the same key features and problems as the original one. Then, optimization is applied to this reduced zonal network taking into account all the selected stochastic scenarios. Subsequently, the resulting zonal expansion plan is transcribed into specific transmission investments.

The proposed methodology is articulated in six steps. First, controllable generation and consumption are calculated with an hourly time step to ensure power adequacy between production and load for each scenario and time horizon (see D8.2.a “Enhanced methodology for the computation of demand/generation scenarios”). At this stage, grid constraints are not taken into account. In a second step, overload problems are detected on a simplified initial pan-European nodal grid. Then, in a third step, the initial network is reduced, leading to a zonal grid. In a fourth step, the modular development plan is calculated at the zonal level considering all time horizons and the whole set of scenarios (see D8.4.a “Enhanced methodology to define the optimal modular plan”). Starting from the zonal modular development plans, the grid expansion is performed for the first two time horizons at a nodal level. Finally, the robustness of the nodal grid architectures is checked to ensure that the expanded networks can be operated without major voltage or stability issues (see D8.5.a “Enhanced methodology to assess robustness of a grid architecture”). This deliverable will focus on steps 2 and 3 which aim at detecting overload problems to reduce the grid to a zonal model. Then, the methodology used for the nodal expansion of the grid, step 5, will be presented in the same document.

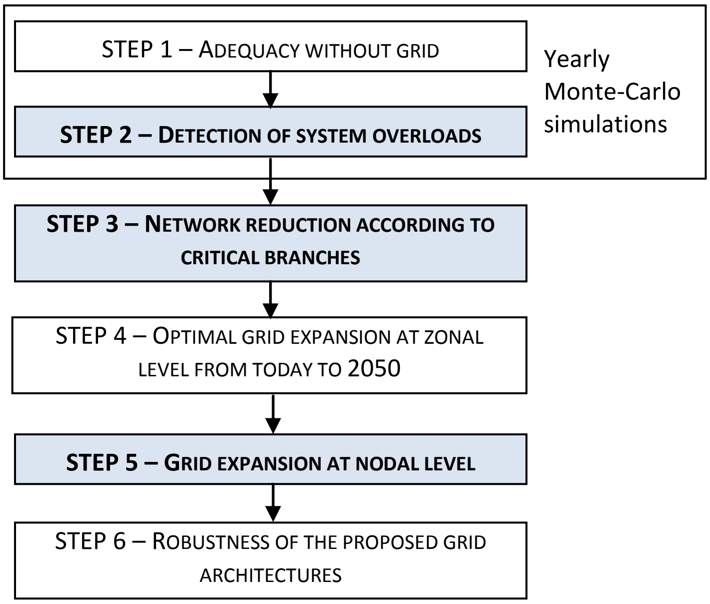

Figure 1. Methodology proposed in e-Highway2050, WP8

This document details parts of this methodology and the results of the case study on which it was applied. First, Section 1 presents the case study on which the proposed methodology was tested. Sections 2, 3, 4, 5 and 6 detail the mechanics of each of the steps 2 to 5 of the methodology except the grid expansion at zonal level, which is presented in a separate deliverable.

The method developed in this report is composed of three main modules:

- The detection of overload problems (Section 4) on a simplified initial 1000-node network, i.e. the quantification of congestion of transmission lines in the initial grid, while using system flexibility in the most efficient way. Flexibility can be brought devices with no operating cost (Phase-Shifting Transformers (PST) or HVDC links), or associated to a cost such as redispatching. In the case of the large European system (around 8,000 nodes), a preliminary network reduction technique is presented in Section 2 to simplify the full grid to 1,000 nodes.

- A network reduction method (Section 5) which calculates an equivalent simplified zonal grid from the nodal system (1,000-node network). This zonal model will be used as the starting point for a modular network development plan. First, the network is split into zones according to identified critical branches, such as frequently congested lines or power flow control devices (PST or HVDC links). Then, a method is proposed to approximate equivalent network characteristics of the original system.

- Finally, a grid expansion technique at the nodal level is described is Section 6. This task aims at finding the optimal nodal expansion plan for the first time horizons where the zonal expansion is common for all scenarios. It consists in identifying the most relevant candidate lines in a first step, and solves the transmission expansion planning problem to select the optimal lines in a second step (using TEPES, a model developed by Comillas).

A detailed review of the main existing approaches to TEP, both in practical settings and in the academic literature, is presented in Appendix A: Existing TEP approaches.

TABLE OF CONTENTS

List of Figures

List of Tables

1. Description of the data used for testing

A simple test case is used to help the integration of the different modules of the WP8 methodology and to test their feasibility. These data are not realistic: they are simply a tool to test the methods and ensure a good integration of all the modules. A final test case of the size of the European system with realistic data will be realized in task 8.6.

This case study is based on a 2012 French-Spanish (FR-ES) HV system where the surrounding countries are modelled as a reduced set of neighbour nodes (see Table I and Figure **2**). The size of this system is similar to the target size of the European system after the initial reduction (from 10,000 nodes to 1,000). Thus, we kept the unreduced FR-ES system in the test case (i.e. the initial reduction step (task 8.3.1) was not performed on the case study). The system includes around 600 generating units with $P_{min} > 0$; their P_{min} and P_{max} have been randomly perturbed, and their generation types have been arbitrarily set to cover all possible types. HMI coordinates of the nodes are available (from a network simulation tool), giving an idea of the geographical distribution of nodes.

Table I – Description of the French-Spanish system used in the test case

Number of nodes	**2196**
Number of external nodes (no FR-ES)	211
Number of 400kV nodes	548
Number of lines	**3715**
Number of 400kV lines	981
Number of 400kV PST	8
Number of 400kV interconnexion lines	45
Number of HVDC lines	0

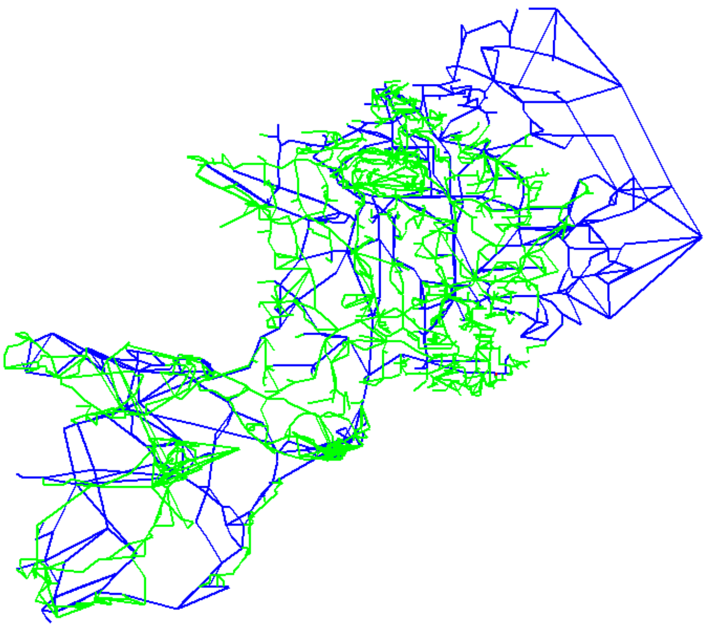

Figure 2. FR-ES system used in the test case (400kV lines in blue; lines <400kV in green)

Then, starting from the 2012 installed capacities and energy mix in both countries (REE, 2013 - RTE, 2013) we built two different scenarios for 2050 according to the following assumptions (Table II):

Table II – Description of the scenario assumptions for 2050

	France	**Spain**
Scenario 1	Decrease nuclear generation	End of nuclear generation by 2050
	Increase wind and solar capacities by a factor 3 by 2050	Increase wind and solar capacities
	Constant load	Increase load by 50% by 2050
Scenario 2	Increase hydro generation	No change in hydro
	Increase gas and coal generation	No change in thermal
	Increase wind and solar capacities by 50% by 2050	Increase wind and solar capacities by 50% by 2050
	Increase load by 30% by 2050	Constant load

In the first scenario, there is a high increase in the Spanish consumption mostly compensated by a large increase in wind and solar generation in France, while only the French consumption is increased in the second scenario. This should result in different flows within the system.

Once the installed capacities of each technology have been calculated for the two scenarios in 2050, values were interpolated for 2030 and 2040. Thus, two different scenarios for three time horizons (2030-2040-2050) are considered in this test case. For each scenario and time horizon, 10 Monte-Carlo years are generated with different samples of the uncertain phenomena such as load, wind and solar. This is done by the module developed in task 8.2 (adequacy simulations without grid). Then, all the methodology is run on this data: DCOPF and detection of critical branches, network reduction (100 zones), snapshot selection, candidate selection, zonal Transmission Expansion Planning (TEP), nodal expansion and robustness study of the proposed architectures.

2. Task 8.3.1: Reduction of the initial network

Detecting overload problems on a large grid is challenging since time complexity is added to spatial complexity. Using the whole existing European network, which includes approximately 8000 nodes, is unrealistic. Moreover, considering the time horizon, it would not be relevant to use the full network. The European grid must be simplified. Existing network reduction techniques mainly aim at keeping branches currently likely to be overloaded and at reducing the other parts of the network. They are not relevant for long-term planning since deep changes in generation and consumption patterns can completely modify the list of such critical branches. Thus, we want to define a method for network reduction based on a criterion unlikely to change by the considered time horizons.

In this subtask, a simple clustering approach for a large transmission network was developed, based on the method presented in Section 5, in order to reduce the complete existing European EHV grid (around 8000 nodes) to around 1000 nodes. Only 400kV nodes are kept in the simplified network and a few nodes which are electrically very close are merged together. Indeed, for a long-term and large scale planning problem, we do not want to look at local issues brought by lower voltage systems, but we want to consider larger phenomena reflected by the very high voltage grid. This simplification is sufficient to reduce the full network to approximately 1000 nodes. Thus, there is no need for a more complex method at this stage.

The resulting grid, called "nodal grid", will be the most detailed grid modelling used in the following tasks. The proposed method uses the electrical distance as a criterion to aggregate the nodes that are electrically close to each other. Additional rules were also introduced in order to take into account phase-shifting transformers (PST), HVDC (High-Voltage Direct Current) links embedded in AC grid and cross-border lines.

Aggregating nodes electrically close to each other implies that very local congestions cannot be detected, which is an acceptable assumption for a continent wide planning methodology. Local reinforcements, if they are necessary, shall be planned in a second stage.

The development of a reduced model comprises two subproblems: the network partition which aggregates the nodes together, and the calculation of the reduced network characteristics. A method is proposed, which is a simplified version of the network reduction method presented in Section 5.

A prototype has been implemented in Matlab.

2.1. Clustering method

In order to reduce the European 8,000-node network to a nodal 1,000-node network, a simplified version of the network reduction method presented in Section 5 has been studied.

The general idea of this simplified method is described in this section, while Section 5 is more detailed.

2.1.1. Preliminary studies

Clustering is the process of grouping the data into clusters so that objects within a cluster have high similarity in comparison to one another, but are very different to objects in other clusters. An appropriate simplified network in long-term planning is therefore a set of clusters (represented by a referent node), where nodes are electrically close to each other within a same cluster and significantly far from nodes in other clusters.

Two clustering methods have been studied and tested. The first one consists in interpreting the problem as a mathematical linear integer program (J. C. Dodu, J. P. Ludot, & J. Pouget, 1969). In this approach, two nodes are defined compatible (resp. incompatible) if the electrical distance between them is below (resp.

above) a certain threshold. Then, the objective function aims at obtaining the minimal number of clusters so that two incompatible nodes are not in the same cluster. However, this method is very time consuming for large networks such as the European one. Besides, by only considering incompatibilities, we lose the electrical distance information. The second studied clustering method is the well-known *K-means* algorithm (Shi Na, Liu Xumin, & Guan Yong, 2010). It has the advantage of being simple and efficient on large sets of data. However, the solution is very dependent on the initial set of centroids.

Therefore we decided to keep the second approach using a heuristic algorithm based on the work presented in Section 5 to build an initial partition close to the optimal one.

2.1.2. Simplified clustering method

Good results from Section 5 being convincing, a simplified version of its method has been developed and is presented here. It is based our on the *K-medoids* algorithm (similar to the *K-means* algorithm, but using data points as centroids) combined with a heuristic algorithm which defines an initial partition close to the optimal one.

It is important to note that only the nodes at the highest voltage level (400 kV) are taken into account in the partition method to avoid distorting the electrical distance and for the reason stated before. The remaining lower voltage nodes are assigned to the geographically closest partition.

A similar heuristic algorithm than the one described in Section 5 is used to build the initial network partition. The network should be split so that end nodes of PST (400kV only), HVDC links and cross-border lines are not in the same cluster. A maximum cluster size is also imposed to have relatively small partitions. Indeed, as we only consider the highest voltage level for the partition, the reduction ratio is very small, as well as the size of clusters. This initial partition is then refined using a modified version of the *K-medoids* algorithm which guarantees that end nodes of PST, HVDC and cross-border lines are never assigned to the same partition. This clustering is done according to the electrical distance (see definition in Section 5). Each partition representative, the medoid, is the node with the lowest average electrical distance to the other nodes in the partition.

Once the final partitions have been calculated and the lower voltage nodes assigned to them, we compute the parameters of the reduced network. Classical network reduction techniques calculate the network parameters of the equivalent corridors so that inter-zonal flows in the reduced network match inter-zonal flows in the nodal network. However, at this stage of the WP8 methodology, we do not have any operational data (simulations are performed on the nodal network). Thus, we compute the reduced network parameters directly by aggregating lines characteristics from the initial network. Admittances and capacities of lines with both end nodes in different clusters are summed to get the equivalent reactances and capacities of the new corridors. This naive method is acceptable as the reduction ratio is small. PST and HVDC lines are considered separately: they are kept in the reduced network.

2.2. Results

We tested this network reduction method on the France-Spain system described in Section 1. This system has 2196 nodes. Thus, we should reduce it to around 250 nodes to keep a similar reduction ratio than the one for the whole European network. The obtained reduced nodal network is displayed on Figure 3.

It should be noted that this reduced nodal grid will not be used in the test case for the following modules, but the starting initial grid (2196 nodes) will be studied instead in order to have a test case of the same size as the nodal European grid.

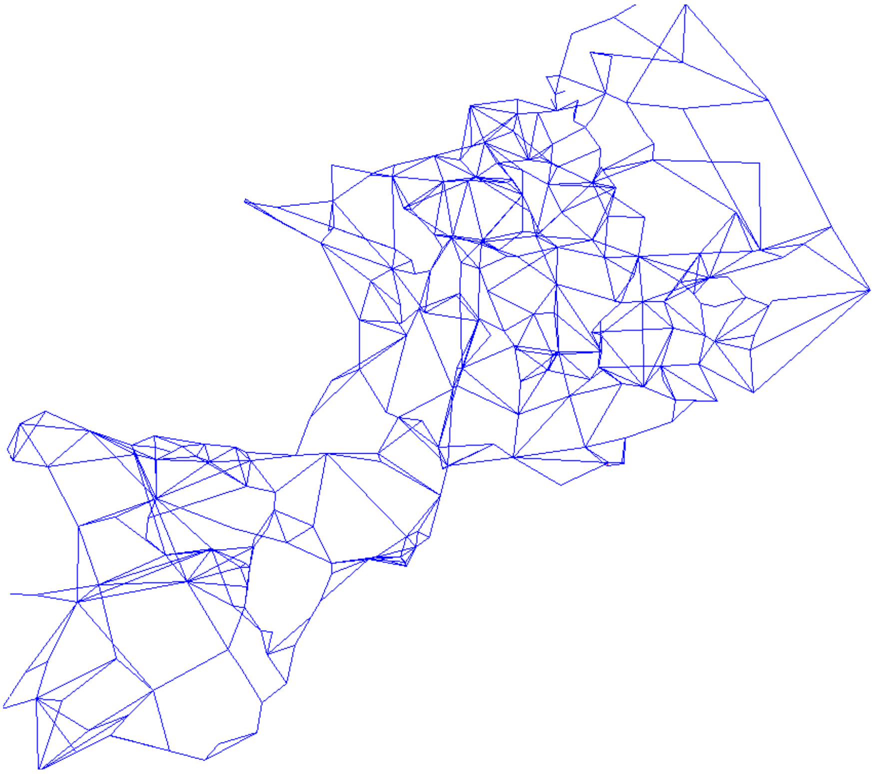

Figure 3. Reduced nodal FR-ES network (250 nodes)

3. Task 8.3.2: Automatic mapping of generation and consumption on nodes

In this module, time series of load and non dispatchable production (solar, wind and hydro Run-Of-River) generated by the adequacy simulations from task 8.2 (see D8.2a) for each country are disaggregated on each node of the simplified 1000-node network. This is performed regarding pre-defined distribution keys for all types of load and generation.

In the WP8 methodology, we suppose that distribution keys for each type of generation are an input of the methodology. Indeed, our goal is not to optimize the generating fleet. The method developed in WP2 (see D2.1 "Data sets of scenarios for 2050") to calculate distribution keys is used to generate the data.

Thus, after adequacy simulations and initial network reduction, there is a simple module which disaggregates time series of load and solar, wind and hydro ROR generation from country or regional level to nodal level according to input assumptions on distribution keys. This is implemented in AMPL.

We should note that dispatchable generating units are allocated on the nodal network before adequacy simulations, and considered independently in the simulations. These units are distributed in the same way than what is done in WP2 (see D2.1 "Data sets of scenarios for 2050").

4. Task 8.3.3: Detection of overload problems (DC OPF)

In this module we want to quantify the congestion of transmission lines in the initial grid, while using system flexibility in the most efficient way. Flexibility can be brought by devices with no operation cost (PST or HVDC links), or associated to a cost such as redispatching.

Detecting overload problems on a large grid becomes challenging since time complexity is added to spatial complexity. Indeed, generation and consumption are defined with hourly time steps for a large number of Monte-Carlo years, for each scenario and time horizon, leading to thousands of injection patterns. One of the challenges is to detect which of these patterns will lead to congestions. We want to solve this problem without selecting ex-ante some representative snapshots, which does not ensure an exhaustive detection of overload problems, especially in a system with increasing uncertainties. In order to detect overload problems, the flows on the simplified nodal grid are computed for all injections using DC Optimal Power Flows (OPF) which take into account the possible network controls (HVDC, Phase Shifter Transformers (PST)). Adequacy simulations in a copperplate system (previous module, see D8.2.a "Enhanced methodology for the computation of demand/generation scenarios") give the optimal dispatch of power plants which minimizes the total system cost. Each adequacy simulation is performed over one year with an hourly time step and a Monte-Carlo approach is used to take into account the stochasticity of load, intermittent renewable generation, hydro inflows and availability of thermal units. Thus, DC OPFs aim at minizing the cost of adjusting controllable generation and load from the optimal dispatch, while complying with network constraints and using in the best way costless controls (HVDC, PST). Each DC OPF is solved independently for each time step. If 2,000 Monte-Carlo years are simulated per time horizon and per scenario, and we consider 7 scenarios and 6 time horizons, this would lead to 735,840,000 DC OPFs. Consequently, the DC OPF model should be simple and solved in a very short time.

Each DCOPF is modelled as a linear optimization problem in which controllable injections, voltage angles, PST phase angles and controllable flows over HVDC links are variables. The objective function is the minimization of the cost arising from the difference between the adjusted and the reference optimal injections. Adjustment costs of controllable generation and consumption have been defined based on priority orders (see Appendix C: Adjustment costs). Generating units are modelled such as shut-down units can be started with an additional cost and hydro power generation stays as close as possible to the reference optimal dispatch. Indeed time dependencies are not taken into account in the DC OPF, so that adjustments of injections implying storage (e.g. hydro power plants with reservoir) should be the smallest.

Finally, each DC OPF returns indicators associated to each transmission line (e.g. flow, congestion duration or marginal cost associated to the maximum flow constraint) and nodes (e.g. marginal price). Then, deciles and average values of these indicators are calculated for each line and each node, and analyzed in order to define *critical branches* and the zonal decomposition (see Section 5).

This DC OPF model has been written in AMPL and is solved using FicoXpress solver (mixed integer solver).

4.1. Mathematical formulation

We consider the simplified European grid from the previous network reduction module, with a set of nodes and a set of transmission lines. Each transmission line is defined by two nodes, which define the sign of the flow. Each generating unit is connected to a node. Demand Side Management (DSM) is aggregated and defined on each node, such as uncontrollable load.

4.1.1. Notations

Indices

i, k, n : Nodes
ik : Branch
N : Set of nodes
B : Set of transmission lines
I : Set of injection types

Parameters

x_{ik} , r_{ik} : Reactance and resistance of branch ik [pu]
I^0_{pin} : Optimal power injection of type i during period p at node n from adequacy without grid [MW]
$sign(i)$: Sign of each injection type i (+1 for power generation and -1 for power consumption)
a_g : Availability of generating unit g, $a_g \in \{0,1\}$
C_{uns} , C_{exc} : Cost of energy not served and cost of energy in excess [€/MWh]
C^+_{pi} , C^-_{pi} : Costs of adjusting (up and down) injections of type i during period p [€/MWh]

Variables

θ_{pn}: Voltage angle during period p at node n
α_{pik} : PST phase angle during period p for branch ik
F_{pik} : Power flow during period p on HVAC link ik [MW]
T_{pik} : Power flow during period p on HVDC link ik [MW]
I_{pin} : Power injection of type i during period p at node n [MW]
δ^+_{pn} : Energy in excess (i.e. production curtailment) during period p at node n [MW]
δ^-_{pn} : Unsupplied energy (i.e. energy not served) during period p at node n [MW]
P_g: Power injection of generating unit g [MW]

4.1.2. Flexible grid devices

In the DC OPF, we want to use at best the possibilities offered by existing flexible grid devices, such as Phase Shifter Transformers (PST) and High-Voltage Direct Current (HVDC) links. Indeed, these possible controls are costless actions which can regulate the flows across the grid. The following paragraphs detail the way they are modelled in the DC OPF.

Phase Shifter Transformers (PST)

A PST is a specialised form of transformer used to control the real power flow on transmission grids and prevent overload. This is done by adding a phase angle which affects the division of power flow between the paths. Taps connections allow controlling the magnitude of the phase shift which takes discrete values between α^{min} and α^{max}.

Let branch ik be an AC transmission line equipped with a PST and let α_{ik} be the PST phase angle. If we consider the expression of real power flow on branch ik under the DC approximation, the previous expression becomes:

$$F_{pik} = B_{pik} \cdot (\theta_{pi} - \theta_{pk} - \alpha_{pik})$$

As we want the DC OPF problem to be linear, the phase angle α is allowed to vary continuously between its bounds α^{min} and α^{max}.

High-Voltage Direct Current (HVDC) link

HVDC links use direct current, so that the power flow can be controlled independently of the phase angle between both ends. Thus, it can vary continuously within its bounds, defined by the maximum permissible flow (i.e. thermal limit).

In the DC OPF, the power flow T_{pik} of an HVDC link ik follows the constraints described below, and is modelled in the balance equation as an exchange on injections, which is illustrated in Figure 4.

$$T_{pik} = -T_{pik}$$

$$|T_{pik}| \leq T_{ik}^{max}$$

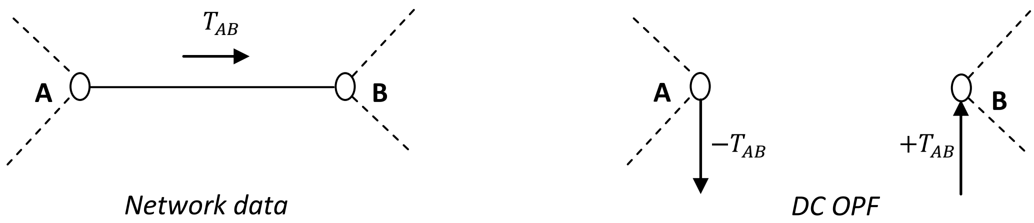

Figure 4. HVDC link model in the DC OPF

4.1.3. Linear optimization

Linear optimization is the problem of maximising or minimizing a linear function over a convex polyhedron specified by linear constraints. It can be expressed in canonical form as:

$$(LP)\begin{cases} \min c^t x \\ \text{subject to } Ax \geq b \\ \text{and } x \geq 0 \end{cases}$$

An Optimal Power Flow problem typically aims at minimizing the power generation costs or the transmission losses in a network subject to physical constraints such as Ohm’s and Kirchhoff’s laws and transmission capacities. This is a classical non linear and non convex optimization problem. Besides, by minimizing transmission losses the objective function becomes quadratic. Consequently, this OPF is computed under the DC approximation (see Appendix B: DC approximation for details on the power flow equations and DC approximation).

In this module, we want to calculate the flows on each transmission line while using at best the grid control devices (HVDC, PST) and remaining as close as possible to the reference optimal dispatch, given by the adequacy simulation without grid. This is equivalent to minimizing the cost of adjusting controllable generation and load relative to the optimal dispatch. As we also want to avoid unbalance in the system, it is also taken into account in the total cost expression. The objective function is:

$$\min_{\theta,\alpha,T,I,\delta} \sum_{N} C_{unbalance} \cdot |\delta_{pn}| + \sum_{N,I} C_{pi} \cdot |I_{pin} - I_{pin}^{0}|$$

The objective function can be linearised by decomposing each variable into two positive variables. For instance, by decomposing δ_n into two positive variables δ_{pn}^{+} (energy in excess) and δ_{pn}^{-} (unsupplied energy) such as $\delta_{pn} = \delta_{pn}^{+} - \delta_{pn}^{-}$, then:

$$|\delta_{pn}| = \delta_{pn}^{+} + \delta_{pn}^{-}$$

We define as well positive adjustment variables up and down for injections, such as:

$$I_{pin} - I_{pin}^{0} = \Delta I_{pin}^{+} - \Delta I_{pin}^{-}$$

The objective function can now be expressed without absolute values, and the DC OPF problem formulated as follows:

$$\min_{\theta,\alpha,T,I,\delta} \left[\sum_{N} (C_{exc} \cdot \delta_{pn}^{+} + C_{uns} \cdot \delta_{pn}^{-}) + \sum_{N,I} (C_{pi}^{+} \cdot \Delta I_{pin}^{+} + C_{pi}^{-} \cdot \Delta I_{pin}^{-}) \right]$$

With the following constraints:

- Balance equation for each node $n \in N$

$$\sum_{i \in I} sign(i) \cdot I_{pin} + \sum_{m \in N} (F_{pmn} - F_{pnm} + T_{pmn}) = \delta_{pn}^{+} - \delta_{pn}^{-}$$

- Transfer capacity constraint for each HVAC transmission line ik and HVDC transmission line jm

$$|F_{pik}| \leq F_{ik}^{max}$$

$$|T_{pjm}| \leq T_{jm}^{max}$$

- PST phase angle constraint for each branch $ik \in B$

$$\alpha_{ik}^{min} \leq \alpha_{pik} \leq \alpha_{ik}^{max}$$

If there is no PST on branch ik, then $\alpha_{ik}^{min} = \alpha_{ik}^{max} = 0$. In order to respect linearity, α_{pik} can vary continuously within its bounds.

- Boundary conditions for each injection type $i \in I$ at node $n \in N$

$$I_{in}^{min} \leq I_{pin} \leq I_{in}^{max}$$

4.1.4. Generating units modelling

Each generating unit is defined by a number, a node to which it is connected, a type (e.g. nuclear or onshore wind generation), maximum and minimum power production bounds, a generation cost, its optimal reference production (from adequacy simulation without grid) and an availability parameter. The unit availability is mainly defined for thermal units and refers to maintenance or outage. It is an output of the Time Series generator in module 8.2 (see D8.2a “Enhanced methodology for the computation of demand/generation scenarios”). This availability parameter a_g is set to 0 if the thermal unit is under maintenance or during an unplanned outage, and it is set to 1 otherwise. However, it does not take into account the unit commitment calculated in the adequacy simulation without grid.

In the DC OPF, we want to allow start-up of shut-down available thermal units. These units have an optimal power production set to zero in the adequacy simulation without grid, but as they are not under maintenance or in outage, they could be started to reduce congestion of branches or ensure adequacy. Thus, three different types of generating units are modelled in the DC OPF:

- Unavailable generating units (maintenance or outage of thermal units): the power production should remain at zero. The unit being unavailable, $a_g = 0$. We define the power production constraint of unit g as follows:

$$a_g \cdot P_g^{min} \leq P_g \leq a_g \cdot P_g^{max} \overset{a_g=0}{\Longleftrightarrow} P_g = 0$$

- Available generating units which are operating in the adequacy simulation without grid: the power production should stay within the minimum and maximum bounds. The power production constraint of unit g becomes:

$$a_g \cdot P_g^{min} \leq P_g \leq a_g \cdot P_g^{max} \overset{a_g=1}{\Longleftrightarrow} P_g^{min} \leq P_g \leq P_g^{max}$$

- Available generating units which are shut-down in the adequacy simulation without grid: the power production may be either equal to zero or vary between P^{min} and P^{max}. As we want to keep the problem linear, the power production variable has to vary continuously within 0 and P^{max}. Thus, if a thermal unit is shut-down in the adequacy simulation without grid, we define the following power production constraint:

$$\boldsymbol{if}\ P_g^0 = 0\ \boldsymbol{then}\ 0 \leq P_g \leq a_g \cdot P_g^{max} \Leftrightarrow \begin{cases} P_g = 0\ \boldsymbol{if}\ a_g = 0 \\ 0 \leq P_g \leq P_g^{max}\ \boldsymbol{if}\ a_g = 1 \end{cases}$$

In the DCOPF, we do not allow to switch hydro PSP units from pumping mode to generating mode (idem for centralised storage).

4.2. Adjustment costs of injections

The adequacy of the power system without grid is simulated in module 8.2 and returns the optimal dispatch with its associated hourly injections for each country and type.

This optimal hourly dispatch is performed in a copperplate system. This dispatch corresponds to the solution that minimizes the overall system cost. Thus, when grid constraints are taken into account this optimal dispatch is unlikely to be feasible, especially in long-term horizons where the network is no longer adapted. Changes in the generation and consumption injections will have to be considered to meet the network constraints. There are two types of changes: increase of generation (resp. decrease of consumption) and decrease of production (resp. increase of load). Each change is associated to an adjustment cost, depending on the hour, the type of the injection and the direction of the change. The distinction between an upward change (increase of injection at a cost c^+) and a downward change (decrease of injection at a cost c^-) is made. Adjustment costs can be negative (e.g. compensation of the fuel not used).

We want to define a way of calculating these adjustment costs so that they represent the difference between the system operating cost from the reference case, in copperplate, and the one from the case with the grid.

The calculation of these costs relies on the definition of a priority order between the different types of generation and consumption. Then, their value should be assessed in order to remain as close as possible to the real system operation. The more controllable a unit is to operate, the less costly it is to adapt its production. In contrast, cutting uncontrollable consumption, commonly known as unsupplied energy, is the most expensive solution for the system. A further study would be interesting to assess whether the resulting congestions are well depicted by these costs in this approach without time-dependent constraints.

Priority orders and adjustment costs are detailed in Appendix C: Adjustment costs.

4.3. Test case results

In the considered case study, 60 Monte-Carlo years are simulated in total (3 time horizons and 2 scenarios, with 10 Monte-Carlo years per horizon and scenario). The adequacy simulator (see D8.2.a), automatic mapping and hourly DCOPFs are run successively for each week of a Monte-Carlo year. This allows us to run the years in parallel. The Linux server we used for the simulations was composed of 16 cores. Thus, we could run up to 16 years in parallel.

The computation times obtained for the adequacy and DCOPFs over one year using FicoXpress solver are presented in Table III.

Table III – Computation times for the simulation of one year in parallel with 15 other years
(*) corresponds to modules developed in task 8.2

Module	**Computation time**
Time series generator*	1min
Hydro scheduling*	10s
Adequacy simulation* (total time for the 52 weekly MILP problems)	20min
Automatic mapping	27min
DCOPFs (total time for the 8736 hourly linear problems)	**1h 22min**
Average running time per year	2h 9min

5. Task 8.3.4: Reduction of the nodal initial grid according to critical branches

The objective of WP8 is to create an enhanced methodology to define large-scale, long-term grid architectures. However, the optimal planning of an area as large as the European system and the uncertainties involved make it impossible to solve the whole problem directly. The strategy developed in WP8 relies on reducing the network to a simpler, equivalent model that is amenable to optimization. Therefore, network reduction methods are necessary to condense the key features of the system into a workable model. This is represented in Figure 5.

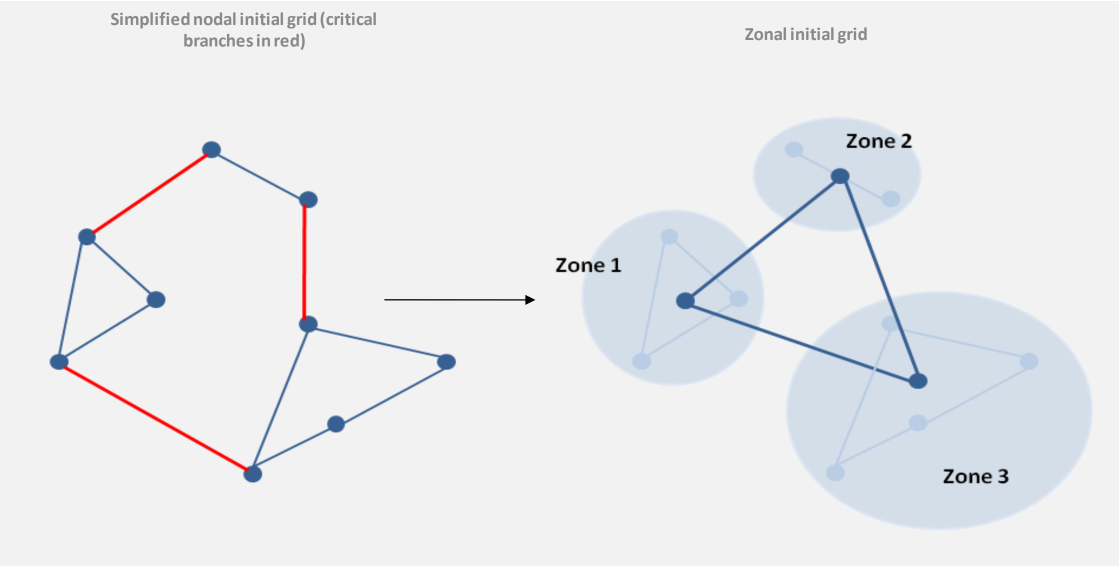

Figure 5. Network partition according to the critical branches

This document describes our proposal for calculating an equivalent simplified zonal network from the nodal system calculated in task 8.3.1 (Section 2). This zonal model will constitute the starting point for a modular network development plan.

We define *critical branches* as the transmission lines that present a special interest for the purposes of TEP. Possible reasons for this special interest are, for instance:

- Frequent congestions. If a line is congested, it will impose operation constraints that would be ignored if the line was internal to a zone. That is particularly important given that congestion is one of the main drivers of transmission expansion decisions. It should be noted that congestions on very short lines are not considered.
- Some power flow control devices, such as HVDC (High-Voltage Direct Current) lines or PSTs (Phase-Shifting Transformers). These elements should be modelled individually in order to capture the flexibility they bring to the operation of the system.

The size of the resulting reduced zonal network (the definition of zones and corridors linking them) must be small enough to be manageable. Otherwise, optimizing the grid expansion over some decades, for several scenarios would not be possible. Although the developed method is flexible in terms of number of nodes, the target size for the European system is about 100 zones for the European System, which we believe to be manageable for TEP but still be able to capture adequately the most important features of the network. Therefore, the objective of this task is to define and develop a network reduction technique able to simplify the model of the European network that has been developed in the initial reduction step in the order of 1000 nodes, to about 100 zones or between 150 and 200 corridors. This reduced network should be able to reproduce the behaviour of the original detailed network with a high enough level of accuracy. This means that, to the extent possible, the inter-zonal flows of the original nodal network, including the flows on the identified critical branches, should approximate those in the equivalent zonal network for all the scenarios and time horizons considered. In addition, given that reducing losses is –together with alleviating congestion and improving reliability– one of the most important drivers of network expansion, it is desirable that the reduced network represents losses adequately.

The development of a reduced model comprises two subproblems:

1. First, *network partition* assigns nodes into zones. This partition should preserve, to the extent possible, all critical branches. That is, the end nodes of critical branches should belong to different zones. Besides, it should assign nodes that are electrically and geographically close to the same partition, in order to keep long corridors in the reduced network.
2. Then, *network reduction* creates a zonal network that approximates the characteristics of the original system as close as possible, including inter-zonal flows and losses.

Ideally, these two subproblems should be performed simultaneously to find the partition that results in the best reduced system. That is, we should solve an optimization problem for network partition and reduction concurrently. However, the unmanageability of this problem leads us to approaching each phase independently. This section reviews the main existing approaches for network partition and describes our proposal for this WP.

This task was first tested on a surrogate case study and then on the WP8 case study. The target number of partitions is established as 50 in order to keep a one-order-of-magnitude reduction in terms of number of nodes.

First, copperplate and transmission-constrained simulations of the European power system allow identifying the most important congestions in the network for a wide set of possible evolutions of the system. These congested lines, together with flow controlling devices such as PSTs make up the *critical branches*, which are used as the key element in the reduction. Once this *reduction based on critical branches* has been performed, the result is a *zonal system* that approximates the behaviour of the complete, original nodal system. The zonal system is small enough to be tractable, but keeps a description of all the relevant congestion of the network thanks to its representation of critical branches.

5.1. Existing approaches for network reduction

Calculating a zonal equivalent network implies two differentiated steps. First, the nodes are assigned to zones by network partition. Then, the parameters that describe the corridors linking zones are calculated. Most of the references that deal with network partition use electrical distance to guide the process. The electrical distance between a pair of nodes in a network is defined as the equivalent impedance between them, i.e., the voltage drop between the nodes when a current of 1 A is transported through the network from one of the nodes to the other. This equivalent impedance is computed using the elements of the inverse of the admittance matrix, i.e., the $Zbus$ matrix (Haixia Wang, Rao Liu, Weidong Li, & Caihong Zhao, 2009). The electrical distance D_{ij} between nodes *i* and *j* is computed as follows:

$$D_{ij} = Zbus_{ii} + Zbus_{jj} - 2Zbus_{ij} \quad (1)$$

where the elements of the matrix $Zbus$ correspond to:

$$Zbus = Ybus^{-1} \quad (2)$$

$$Ybus_{ij} = -\left(R_{ij} + \mathrm{j}X_{ij}\right)^{-1} \quad (3)$$

$$Ybus_{ii} = \sum_j \left(R_{ij} + jX_{ij}\right)^{-1} + \sum_j \mathrm{j}B_{ij,i} \qquad (4)$$

where *R*, *X*, *G* and *B* represent the resistance, reactance, conductance and susceptance of the corresponding lines, respectively.

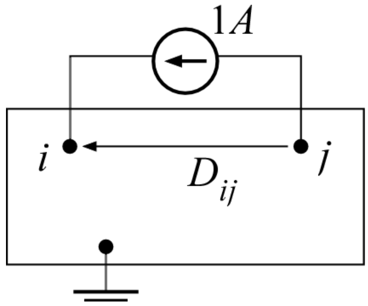

Figure 6. Calculation of the electrical distance between nodes *i* and *j*. The distance reflects the voltage drop between the nodes when a current of one unit is injected in one of the nodes and withdrawn in the other.

Distances between pairs of nodes that are electrically connected by short, low reactance, lines are shorter than distances between nodes that are only connected indirectly through high equivalent impedances. It is important to note that it is necessary to include the conductances and susceptances of all system lines in the calculation in order to avoid having a singular, noninvertible, matrix $Ybus$.

Electrical distance is not the only distance measure we can use. When defining this measure, we can make other considerations, some of which are described below. Once this distance measure has been defined, we need to find the partition (that is, the assignment of nodes to zones) that minimizes the aggregate intra-zonal distance and, in the cases where the number of zones has not been determined, maximizes the inter-zonal one. Mixed-Integer Programming (MIP) can model this as an optimization problem. However, solution times can be unmanageable even for small-sized networks (Hamon, Shayesteh, Amelin, & Söder, 2014), and, therefore, this technique is difficult to apply to real-size systems. Other approaches include the application of spectral partitioning (Hamon et al., 2014), a technique that is widely used in image segmentation. This method is based on the computation of the eigenvalues of the similarity matrix (which expresses the distance between variables). These eigenvalues are then used to reduce the dimensionality in the attributes before applying a clustering algorithm. Alternatively, other authors identify clusters of nodes based on electrical distance using classical clustering algorithms such as *K-means* or *K-medoids* (Cotilla-Sanchez, Hines, Barrows, Blumsack, & Patel, 2013). This approach has the advantage of being efficient over large sets of data and constitutes the basis of the proposed technique.

However, if network partition is established solely on the basis of electrical distance, all considerations other than network topology are disregarded. No information about the operation of the system, the placement of generation and demand, or the capacities of lines is taken into account. More importantly, there is no guarantee that frequently congested lines will not belong to the same partition, potentially leading the planning process to miss some important reinforcement needs. In addition, using electrical distance can sometimes result in partitions that are in conflict with the intuitions that TSOs can derive from geography alone. The approach we propose and implement in e-Highway2050 is based on combining the information contained in electrical and geographical distances calculated, and incorporating constraints related to the representation of critical branches in the reduced network model. In addition, we propose a heuristic algorithm that builds a partition that will be used as the starting point of the clustering algorithm. This initial partition has the added interest of showing the simplest partition that is able to maintain the explicit representation of all the transmission lines labelled as critical.

5.2. Identification of critical branches

As mentioned above, the most relevant transmission lines for the operation of the system will be labelled as critical branches. In addition, some other critical branches will be identified by the analysis of operation scenario data. We propose several criteria for the identification of these branches:

- **Average flow** above a threshold percentage of its capacity, which captures the utilization of a transmission line. Average absolute flow (that is, average flow as a percentage of capacity) captures concisely the utilization of a transmission line.
- However, even if a line supports a high average flow, increasing its capacity will not generally result in operation savings unless the line is already congested. Therefore, we propose to use the **proportion of operation hours where the line is congested** as an indicator to complement average flow. If this proportion exceeds a certain threshold, the line is considered a critical branch.

The economic impact of congestion in two different lines can be very different. In order to filter the congested branches with the highest economic consequences, we propose to analyze the marginal value of capacity and admittance in each line. Based on reference (Olmos, Rivier, & Cabezudo, 2013), the marginal value of a line can be calculated as:

- If the line is congested, the absolute value of the nodal price difference between the extremes of the line weighted by duration.
- If the line is not congested, the absolute nodal price difference scaled by the relative line flow (the flow divided by its capacity).

Inspired by these definitions, we propose the following two indicators:

- The value of the **dual variable of the capacity limit constraints** considered when solving the power flow, weighted across periods and scenarios.
- **The difference between the nodal prices** at the extremes of the line weighted with the line flow across periods and scenarios.

The indicators above have the advantage of incorporating the effect of both congestion and losses. A filter is first applied to remove very short lines from the critical branches selection.

Once calculated in the case study, we found that there was a considerable overlap among indicators. The branches that are congested a large proportion of scenarios tend to have a high average relative flow and high congestion severity indicators. Even though the critical branches that were selected differ with the criterion, the problem areas they highlight are basically the same as shown in Figure 7.

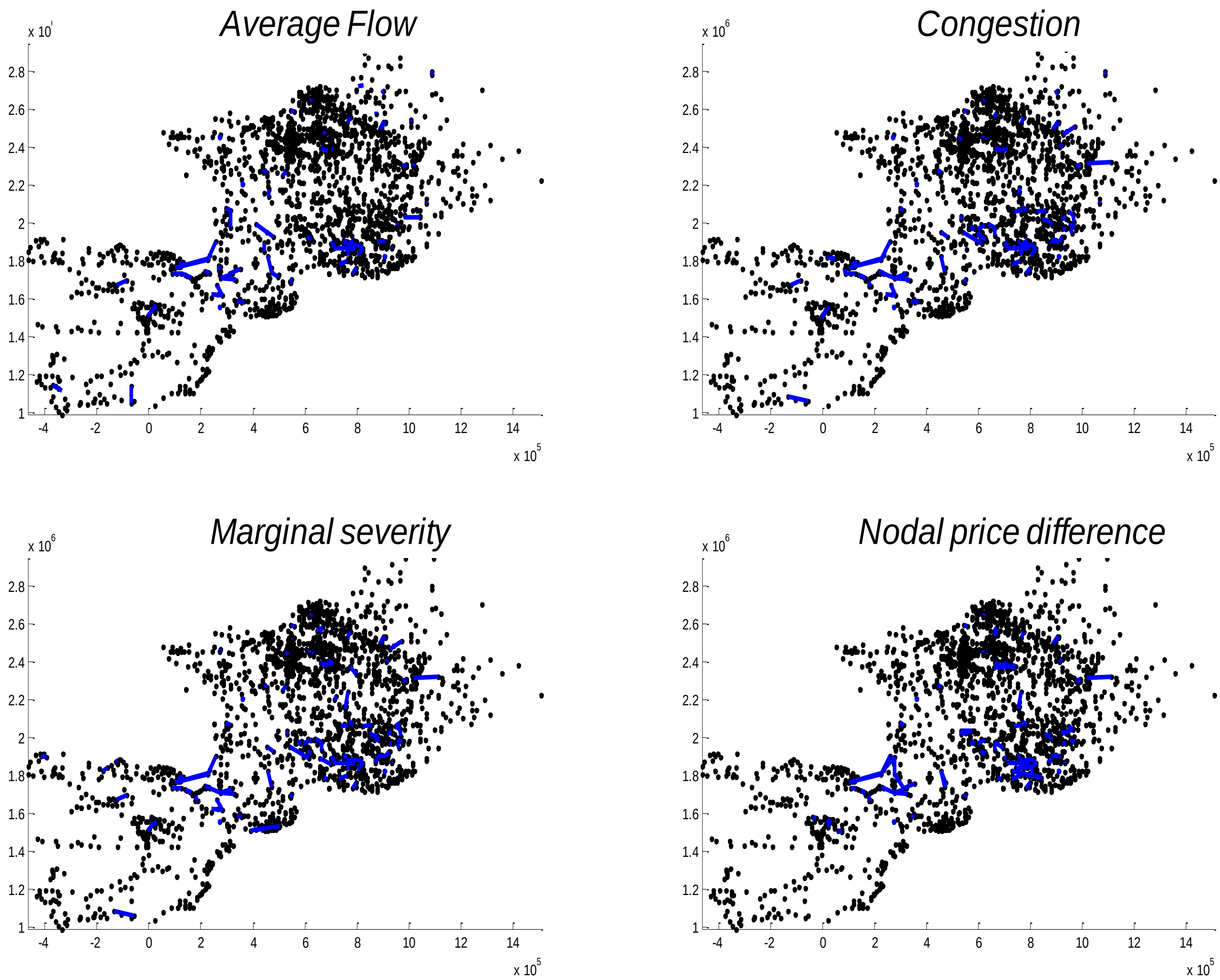

Figure 7. Critical branches (represented in blue) according to the different criteria.

5.3. Distance definition

We propose to base network reduction on a composite distance that is calculated as a weighted average of several individual distances. In this way, we can incorporate additional considerations into the analysis. For instance, including geographical distance ensures that geographically compact partitions are favored. Other economic considerations can be taken into account in the definition as well, such as average Locational Marginal Prices (LMPs), so that nodes with similar prices have a higher probability of being clustered together. Alternatively, we can use Power Transfer Distribution Factors (PTDFs) with respect to critical branches, so that the nodes where a power injection or withdrawal has a similar effect on the flow in critical branches have a higher probability of being clustered together. Although other definitions, as seen above, are possible, in the case study we favor electrical distance combined with a geographical one. Electrical distance captures the structure of the network, while combining it with the geographical one ensures that geographically compact partitions are obtained. LMPs are to some extent considered in the definition of critical branches, given that frequently congested transmission lines related to relevant congestion from an economic point of view tend to have large differences between the LMPs of their extreme nodes, and, therefore, to be selected as critical branches. It is also important to note that only the highest voltage level in the network is taken into account in the partition mechanism, in this case 400 kV, to avoid distorting the electrical distances. The remaining lower voltage nodes are assigned to the geographically closest partition. However, the nodal network should only contain 400kV nodes if it has been reduced following the method in Section 2.

5.4. Initial network partition

The heuristic algorithm builds an initial partition by starting with a single zone that is potentially split as many times as critical branches have been identified:

- If both extremes of a critical branch belong to the same zone, this zone is split in two new zones.
- The nodes that belong to the split zone are reassigned to the subzone, between the two created, that is closest to these nodes in terms of composite distance.

This simple algorithm ensures that critical branches are represented explicitly in the partition and incorporates all the information that has been considered relevant for the composite distance calculation. This initial partition is subsequently refined by a clustering algorithm.

The application of the initial network partition to the case study can be seen in Figure 8Figure 7. This initial partition needs only 24 zones in order to define all critical branches explicitly.

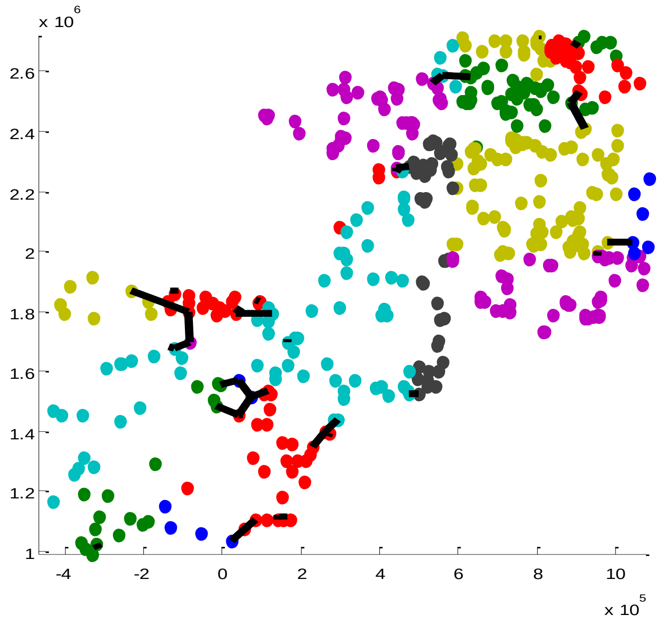

Figure 8. Initial partition according to critical branches (thick, black lines).

5.5. Refining the partition

Most of the few works that tackle network partition explicitly apply *K-means* or *K-medoids* to cluster the nodes into zones according to electrical distance (Blumsack, Hines, Patel, Barrows, & Cotilla Sanchez, 2009; Cotilla-Sanchez et al., 2013). We use a modified version of *K-medoids* that avoids assigning both end nodes of a critical branch to the same zone. *K-medoids* refines the partition by applying the following steps iteratively (Hartigan & Wong, 1979):

- The algorithm chooses a representative node for each zone, the *medoid,* which presents the lowest average distance to the rest of nodes within the zone.

- The algorithm updates the partition by assigning each node to the zone whose medoid is closest in terms of composite distance. This step has been modified with respect to classical implementations of *K-medoids* to guarantee that the end nodes of a critical branch are never assigned to the same zone.

This is exactly equivalent to the better known *K-means* algorithm except in the selection of the representative node. In the case of *K-means* the representative is calculated as the mean of the nodes in the partition. On the contrary, *K-medoids* chooses the node with the lowest average distance to the remaining nodes in the partition.

The medoids calculated in this way have the disadvantage of often being relatively small, not particularly remarkable nodes.

Thus, we propose an alternative criterion for the definition of the final representative node of each zone: the *most connected node.* We define it as the node that has the highest connection capacity to the rest of the network. This guarantees that the representatives will be relatively important nodes in the network, such as large power plants or highly connected substations. In order to guarantee that the representative node of each zone is a central node with enough connections relatively to the others, another solution could be to weight these two criteria.

The resulting partitions and the medoids are represented in Figure 9, Figure 10 and Figure 11.

The starting partition is subsequently refined by the proposed modified *K-medoids* algorithm. In order to appreciate the impact of the definition of the composite distance, two partitions are provided below. Figure 9 corresponds to using the electrical distance, while Figure 10 uses a composite distance that is built as 50% electrical and 50% geographical distance. Although the differences are subtle, the second case avoids some of the problematic zone definitions that can arise if only electrical distance is used, where several zones overlap geographically.

The connectivity map for the system is shown in Figure 11, where nodes are displayed with a size proportional to their connectivity. As can be seen, a large proportion of nodes have a relatively low connectivity to the rest of the network. The final result of the reduction is shown in Figure **12**. This zonal network is now small enough to be tractable for network expansion planning purposes.

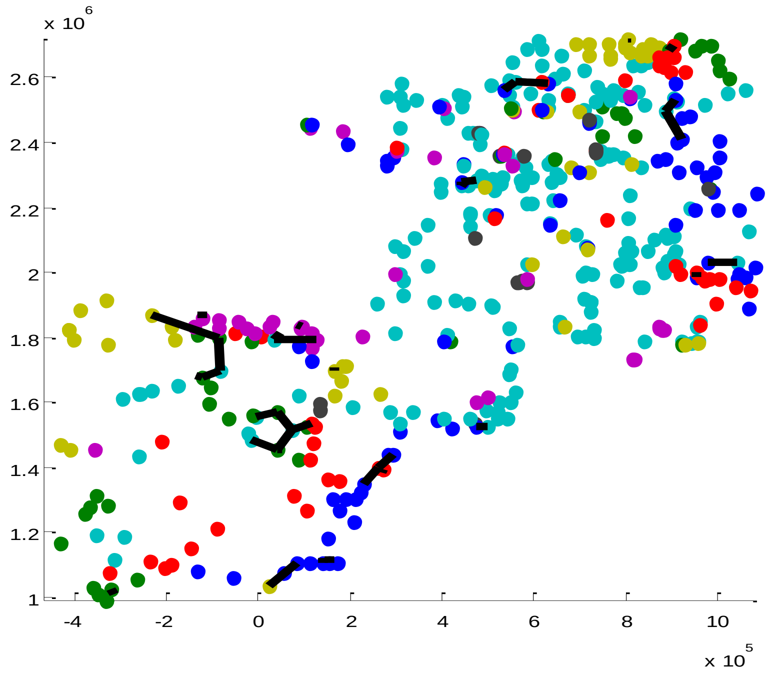

Figure 9. Network reduction for the case study using 100% electrical distance.

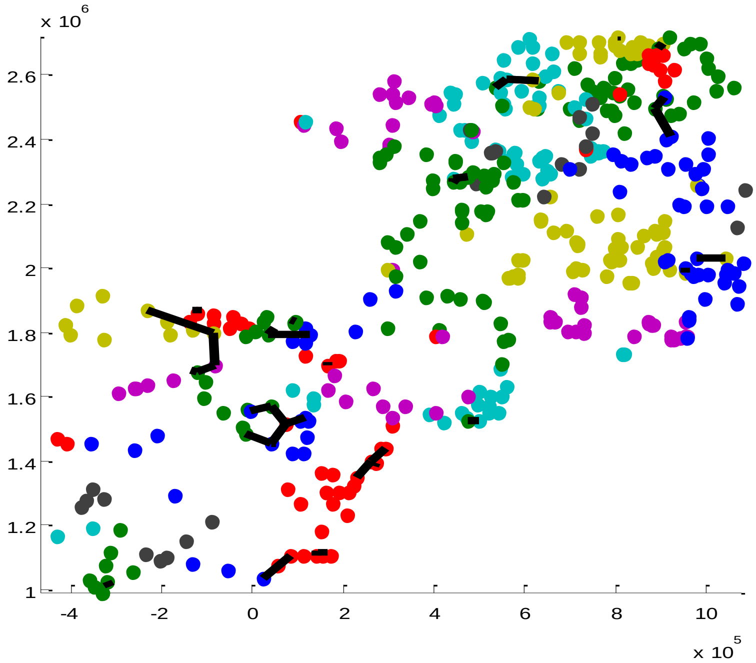

Figure 10. Network reduction for the case study using a 50% electrical and 50% geographical distance.

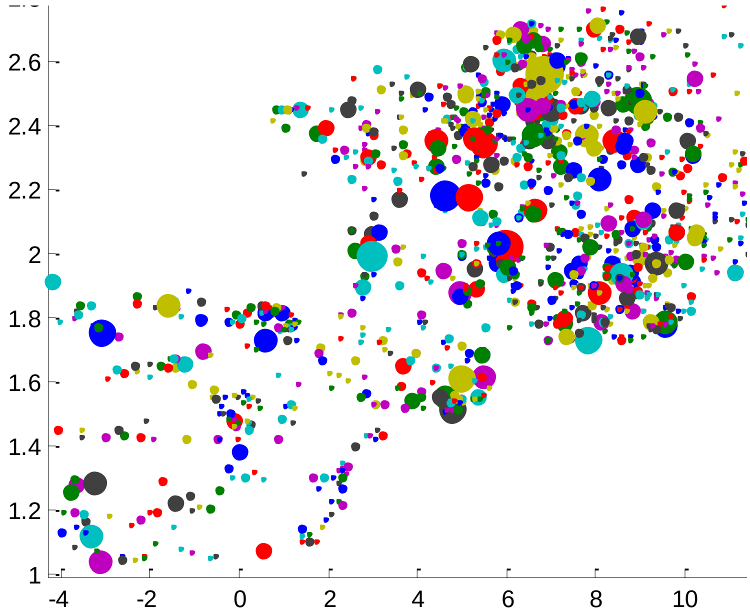

Figure 11. Connectivity map of the system. Nodes are given a size that is directly proportional to their connectivity. Colours were used for the sake of clarity.

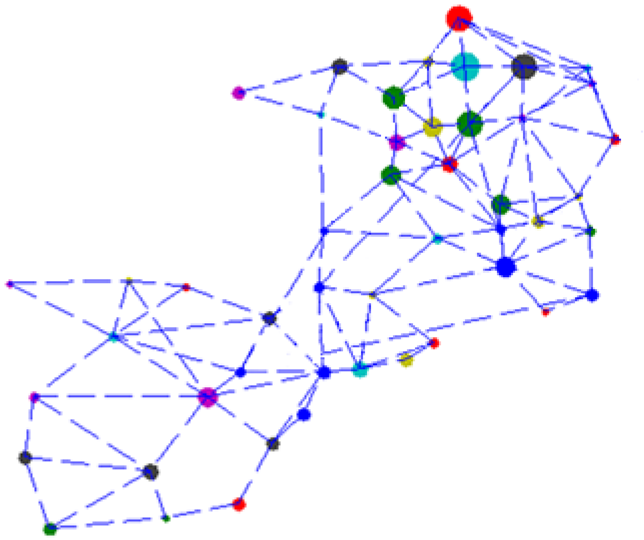

Figure 12. Representation of the reduced network

5.6. Calculation of network parameters

Once the zones in the reduced (equivalent) network have been computed, we need to calculate the parameters that describe the corridors among them. These parameters are the equivalent reactances and physical capacities of the corridors of the reduced network. The objective is to compute a unique reduced equivalent network. Therefore, the parameters computed must be unique, that is, they must be independent of the operation situations.

Classical network reduction techniques divide the network into internal buses and external buses. Among the internal buses, those of them that have branches connecting both external and internal buses are called boundary buses. Classical techniques assume that the internal network is known, the external network is remote and has a limited influence on the operation of the internal network and, finally, that the number of boundary buses is small compared to the number of internal buses.

For this task, we follow an approach based on reference (Shi & Tylavsky, 2012), where the authors define inter-zonal corridors as the equivalents of the sets of lines connecting pairs of zones in the nodal network model. These inter-zonal corridors are both the critical and not critical braches previously used for the network reduction.

The main idea followed to calculate the network parameters of the corridors is that inter-zonal flows in the reduced network must match the inter-zonal flows in the nodal network. Due to the different characteristics of the equivalent reactances and physical capacities of the corridors, we have employed two different methodologies to compute them.

5.6.1. Methodology to compute network reactances of corridors

The purpose of this sub-section is to describe the methodology employed to compute the reactances of the inter-zonal corridors in the reduced network. As previously mentioned, we followed the approach proposed in (Shi & Tylavsky, 2012).

The authors in (Shi & Tylavsky, 2012) proposed to determine the reactances of the inter-zonal corridors so that the differences in the inter-zonal flows in the existing nodal network and in the reduced equivalent network are minimized, as expressed in equation (5). Contrary to what happens in other reduction approaches, the proposed technique minimizes errors in inter-zonal flows for multiple scenarios simultaneously. Thus a single reactance is computed for all scenarios.

$$\begin{aligned} &\min \left\| F^{zonal}_{nodal} - F^{zonal}_{zonal} \right\| \\ &x^{zonal}_{i} \neq 0 \forall i = 1, \dots, L^{zonal} \end{aligned} \qquad (5)$$

The reactances of the inter-zonal corridors can be calculated solving a system of linear equations that makes use of the PTDF matrix of the reduced network. Thus, the first step is to compute this PTDF matrix. The PTDF matrix of the zonal network, $PTDF^{zonal}$, can be expressed as a function of the aggregate power injections in the zones, P^{zonal}_{inj}, and the inter-zonal flows, F^{zonal}, which are both known from the nodal network. By operating these expressions, the PTDF matrix of the zonal network can be expressed as a function of the PTDF matrix of the nodal network ($PTDF^{nodal}$), the topology of the nodal network and the assignment of nodes to zones, as expressed in (6).

$$PTDF^{zonal} = \Pi_f PTDF^{nodal} diag\left(P^{nodal}_{inj}\right)\Gamma\left[diag\left(P^{zonal}_{inj}\right)\right]^{-1} \qquad (6)$$

where Π_f is the matrix of correspondences of lines in the nodal network with the corridors in the reduced zonal network; Γ is the matrix of correspondence of nodes to zones and P^{nodal}_{inj} are the nodal power injections in each node.

The next step is to obtain the reactances that may reproduce, in the most accurate way, the PTDF matrix of the reduced network previously obtained. Equation (7) relates the reactances of the corridors with the PTDF of the zonal network.

$$PTDF^{zonal} = diag\left({}^{1}/_{x^{zonal}}\right) C^{zonal} \left[C^{zonal^t} diag\left({}^{1}/_{x^{zonal}}\right) C^{zonal}\right]^{-1} \qquad (7)$$

where x^{zonal} are the reactances of the reduced zonal network and C^{zonal} is the zone-corridor incidence matrix, which only depends on the topology of the reduced network. Operating (7), we may obtain equations (8)-(9).

$$\begin{bmatrix} N_m \\ \Lambda \end{bmatrix} \left({}^{1}/_{x^{zonal}}\right) = \begin{bmatrix} F^{zonal}_{ij} / \theta^{*}_{ij} \\ 0 \end{bmatrix} \qquad (8)$$

$$\Lambda = \begin{bmatrix} \left(PTDF^{zonal} C^{zonal^t} - I\right) diag(c_1) \\ \vdots \\ \left(PTDF^{zonal} C^{zonal^t} - I\right) diag(c_i) \end{bmatrix} \qquad (9)$$

where N_m is a $1 \times L^{zonal}$ matrix with element in m position equal to one and the other elements equal to zero; F^{zonal}_{ij} the power flow between zones i and j; θ^{*}_{ij} is the average angular differences between the nodes in zones i and j, I is the identity matrix and c_i are the column vectors that represent matrix C^{zonal}.

Solving equation (8) the values of the reactances x^{zonal} of the interzonal-corridors are obtained.

Illustration on a small test case: 9 nodes – 3 zones

In order to illustrate the methodology developed to compute the equivalent reactances of corridors, a small test case will be used. A 9-Bus power system will be reduced to an equivalent 3-Zone power system. The schematic representation of the power system and the reduced network that would be obtained are displayed in Figure 13. Network data of the test case is indicated in Table **VII**.

Table IV – 9-Bus network data

Line	Reactance [p.u.]	Capacity [MW]
1-2	0.0580	500.00
1-4	0.0400	500.00
2-3	0.0340	150.00
2-4	0.0800	500.00
2-5	0.0400	150.00
2-6	0.0400	100.00
3-5	0.0200	500.00
3-8	0.0800	500.00
4-6	0.0200	100.00
5-6	0.0200	100.00
5-8	0.0800	500.00
6-7	0.1200	500.00
6-9	0.0400	500.00
7-9	0.0400	500.00

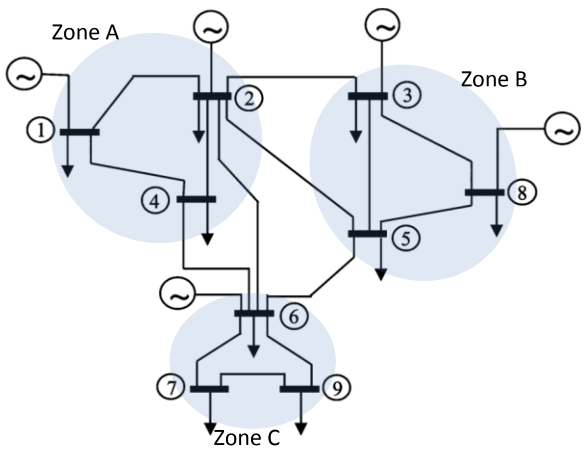

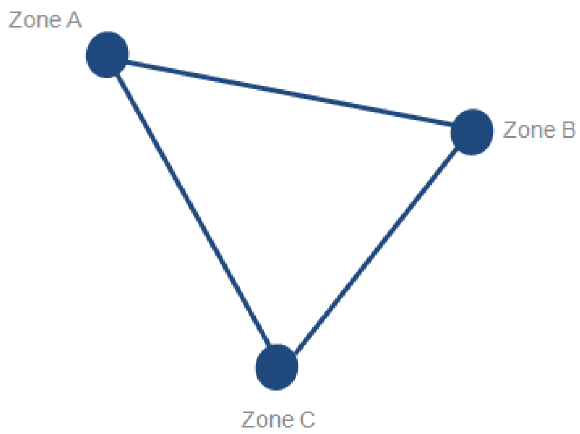

Figure 13. 9-Bus schematic representation and 3-Zone equivalent network.

The equivalent reactances obtained using the methodology explained in this section are indicated in Table **V**. It is remarkable to see that the power flows obtained using the zonal network (with the equivalent reactances previously computed) are equal to the inter-zonal power flows of the nodal network, which was the objective of the methodology. It is also interesting to see that the corridor B-C, which is only composed of line 5-6, has an equivalent reactance (0.0267 p.u.) different to this line (0.0200 p.u.). This happens because for computing the equivalent reactance of the corridors, the methodology also considers the reactances of the inter-zonal lines.

Table V – Inter-zonal corridors with their equivalent reactances and the inter-zonal power flows obtained using the nodal network and the equivalent network.

Corridor	Reactance [p.u.]	Inter-zonal flows obtained using nodal reactances [MW]	Inter-zonal flows obtained using equivalent reactances [MW]
A-B	0.0179	-111	-111
A-C	0.0216	-17	-17
B-C	0.0267	60	60

5.6.2. Methodology to compute equivalent physical capacities of corridors

The purpose of this sub-section is to describe the methodology employed to compute the equivalent physical capacities of the inter-zonal corridors in the reduced network. Due to the lack of references, we have developed a method with this specific purpose. The main idea is that capacities of inter-zonal corridors in the reduced network must allow the maximum transfer of power among zones that may occur in the existing nodal network. In other words, the capacities of the inter-zonal corridors must permit all the inter-zonal flows that may occur in the nodal network.

In the case of a nodal network (Figure 14), the physical capacity between two connected nodes is normally the thermal limit of the line connecting them. If we consider that the parallel lines between N2 and N3 are identical ($C_2 = C_3$ and $Z_2 = Z_3$), the equivalent physical capacity between them is the sum of the thermal limits: $C_2' = 2\,C_2$. If we now consider a more general case where the parallel lines have different reactances and thermal limits ($C_2 \neq C_3$), the equivalent physical capacity between N2 and N3 is calculated so that it allows the maximum possible flow between N2 and N3:

- If $Z_2 C_2 < Z_3 C_3$, then $C_2' = C_2 \cdot (1 + {}^{Z_2}/_{Z_3})$
- If $Z_2 C_2 > Z_3 C_3$, then $C_2' = C_3 \cdot (1 + {}^{Z_3}/_{Z_2})$

Thus, the equivalent physical capacity between N2 and N3 depends on the characteristics of the lines connecting them.

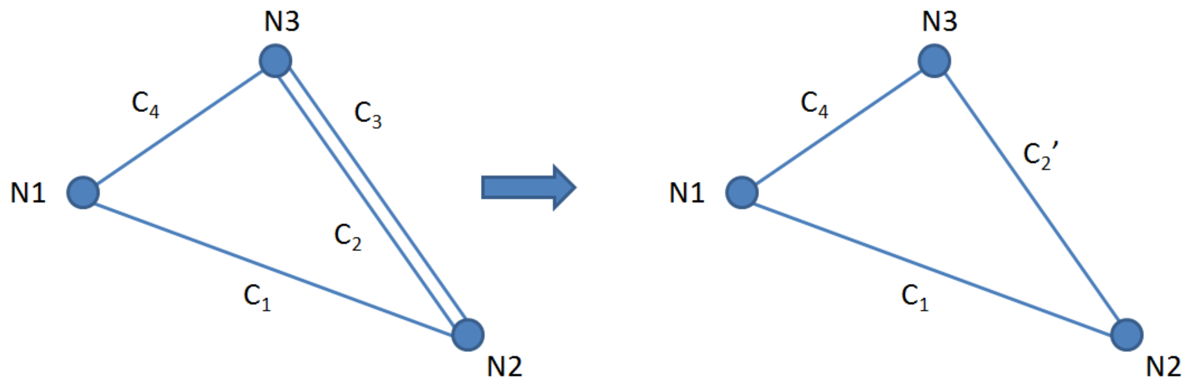

Figure 14. Calculation of corridor equivalent capacities in a nodal network (where C_i are the thermal limits)

However, the case of an equivalent network is more complicated. The sum of the capacities of lines connecting two zones gives a maximum bound of the equivalent inter-zonal physical capacity, but this strategy does not consider the phenomena of potential uneven loads of the different lines at the interface (due to clustering, lines start and end at different substations, see Figure 15) and thus cannot be applied without resulting in a possible overestimation of the equivalent capacities. Moreover, there is no guarantee that the maximum transfer capacity of an inter-zonal corridor is the same in both directions ($A \rightarrow B$ and $B \rightarrow A$).

Another point that should be kept in mind is whether or not N-1 system reliability should be considered while computing the equivalent physical capacities, i.e. if the impact of a line outage on a line should be taken into account in the calculation. In the WP8 methodology, it has been chosen to ensure N-1 system reliability at the nodal expansion step, but not in the former steps (see D8.10 "High-level definition of a new methodology for long-term grid planning"). Thus, N-1 contingencies are not considered at the zonal level.

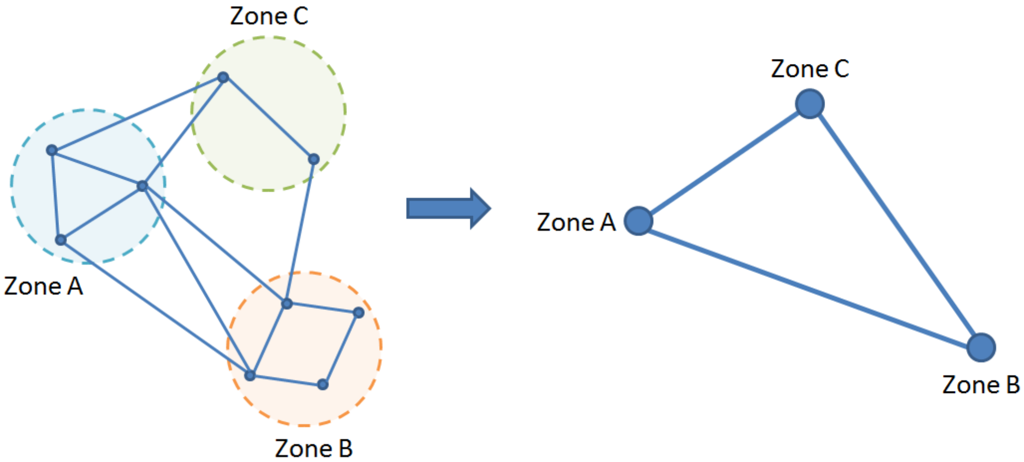

Figure 15. Illustration of an equivalent network from a nodal one

The proposed method is one alternative among others that adapts better to the requirements of the overall methodology. However, if another method would appear to have proven better properties, it would be very easy to switch to this method, without impacting the rest of the methodology.

Compute maximum physical capacity for each inter-zonal corridor

The maximum physical capacity for a given inter-zonal corridor reflects the maximum power that may be transfered through the corridor while respecting each thermal limit of each tie line composing the inter-zonal corridor. In order to compute it, several operation situations were considered, which are meant to represent a variety of stressed operation situations in the system. Snapshots are selected over all the simulated DCOPFs (all scenarios, time horizons and Monte-Carlo years) and correspond to operation situations where tie lines between zones are constrained.

Using these snapshots as the base cases, we simulate the increase of transfer of power between each pair of zones over the selected snapshots until reaching a limit on a line connecting both zones, as depicted in Figure 16. Maximum transfer of power among zones A and B in the nodal network. For this purpose, we use the nodal PTDF matrix and increase homothetically generation and demand of the nodes in the exporting and importing zones until a nodal network limit is reached in the inter-zonal corridor.

In the following paragraphs, we consider that zone A is the exporting zone and E is the set of nodes within this zone (i.e. exporting nodes), while zone B is the importing zone and I is the set of nodes within this zone (i.e. importing nodes). We define $A \rightarrow B\ lines$ the set of tie lines composing the inter-zonal corridor between zones A and B.

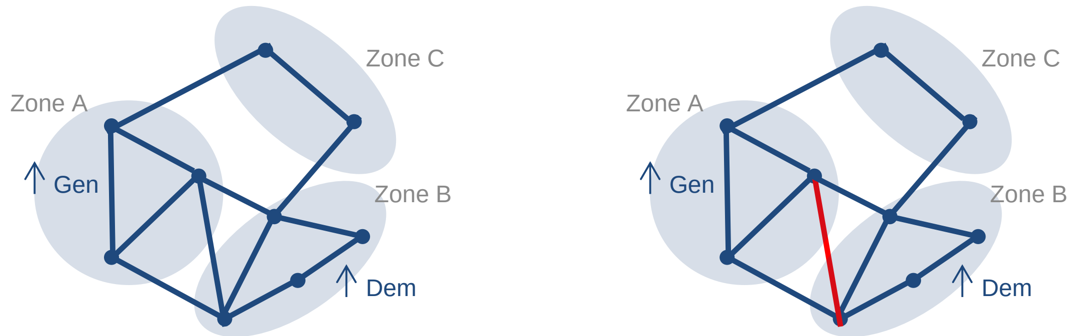

Figure 16. Maximum transfer of power among zones A and B in the nodal network

The optimization problem presented in (10)-(17) is used to modify the base case, snapshot p, and increase the transfer of power between two zones (A to B) until a limit is reached on a tie line composing the inter-zonal corridor between A and B. Then, the resulting power flow $A \rightarrow B$ on this corridor is calculated using the zonal $PTDF$ matrix (previously computed) and the aggregated injections obtained in the optimization problem. This $A \rightarrow B$ flow is kept and compared to the ones obtained from the other base cases: the equivalent $A \rightarrow B$ physical capacity corresponds to the maximum inter-zonal flow.

$$\max \sum_{ne \in E} \Delta gp_{ne}^{p} \tag{10}$$

subject to:

$$\sum_{ne \in E} \Delta gp_{ne}^{p} = \sum_{ni \in I} \Delta d_{ni}^{p} \tag{11}$$

$$inj'_{nd,p} = INJ_{nd,p}^{0} + \Delta gp_{nd}^{p} - \Delta d_{nd}^{p} \qquad \forall nd \tag{12}$$

$$f'_{l(ij),p} \leq \overline{F_{l(ij)}} \qquad \forall l(ij) \in A \rightarrow B \; lines \tag{13}$$

$$-f'_{l(ij),p} \leq \overline{F_{l(ij)}} \qquad \forall l(ij) \in A \rightarrow B \; lines \tag{14}$$

$$f'_{l(ij),p} = \sum_{nd} PTDF_{l(ij)}^{nd} inj'_{nd,p} \qquad \forall l(ij) \tag{15}$$

$$\Delta gp_{ne}^{p}\left(1 - {GP_{ne}^{0}}\Big/{\sum_{ne} GP_{ne}^{0}}\right) = {GP_{ne}^{0}}\Big/{\sum_{ne} GP_{ne}^{0}} \sum_{nee \neq ne} \Delta gp_{nee}^{p} \qquad \forall ne \in E \tag{16}$$

$$\Delta d_{ni}^{p}\left(1 - {D_{ni}^{0}}\Big/{\sum_{ni} D_{ni}^{0}}\right) = {D_{ni}^{0}}\Big/{\sum_{ni} D_{ni}^{0}} \sum_{nii \neq ni} \Delta d_{nii}^{p} \qquad \forall ni \in I \tag{17}$$

where Δgp_{ne}^{p} is the increase in power production in node ne; Δd_{ni}^{p} is the increase in the power consumption in node ni; E and I are the set of nodes labelled as exporting and importing nodes, respectively; $inj'_{p,nd}$ is the power injection resulting when adding the increase in the power production and consumption in node nd; $INJ_{p,nd}^{0}$ is the current power injection in node nd in snapshot p; $f'_{p,l(ij)}$ is the power flow through line l, connecting nodes i and j; $\overline{F_{l(ij)}}$ is the thermal limit of line l; $PTDF_{l(ij)}^{nd}$ is the element located in row $l(ij)$ and column nd of the $PTDF^{nodal}$ matrix; GP_{ne}^{0} is the power production in node ne in snapshot p and D_{ni}^{0} is the power consumption in node ni in snapshot p.

Equation (10) is the objective function of the optimization problem, which maximizes the increase in power production over the exporting nodes, i.e. in zone A (and therefore, the increase in power consumption over the importing zones, i.e. in zone B, as indicated in (11)). Equation (11) indicates that the increase in power production over the exporting nodes must be equal to the increase in the power consumption over the importing nodes. Equation (12) defines the new power injection in each node as the power injection in the base case adding the increase in power production and subtracting the increase in power consumption. Equations (13)-(14) are the upper and lower bounds of the power flow through each line $l(ij)$ composing the inter-zonal corridor between zones A and B, and equation (15) defines the power flow of each line $l(ij)$ of the nodal network based on the $PTDF$ matrix and power injection in each node of the network. Equations (16)-(17) defines the increase in power production/consumption of each exporting/importing node as proportional to the power production/consumption of these nodes in the base case. In the exporting zone, we compute the percentage of the total power production in the zone that corresponds to every node that is producing power ($GP_{ne}^0 / \sum_{ne} GP_{ne}^0$) and, similarly, we compute the percentage of the total power consumption in the zone that corresponds to every node that is consuming power ($D_{ni}^0 / \sum_{ni} D_{ni}^0$).

The increase of generation and demand in these nodes is done homothetically to these percentages, while the remaining nodes in the network are not able to increase generation or consumption.

Using this formulation, the computation of the physical capacity of an inter-zonal corridor is only affected by inter-zonal constraints of tie lines composing the considered corridor (equations (13)-(14)). Indeed, we do not want intra-zonal congestions to size the maximum inter-zonal physical capacities: these intra-zonal congestions will be solved later in the nodal expansion (see Section 6). It can be noted that if critical branches are well selected, intra-zonal physical capacities should not be limiting. Moreover, we do not want congestions on inter-zonal lines which do not directly connect zones A and B to size the $A \to B$ inter-zonal corridor capacity. This would underestimate the physical capacity between zones A and B in the zonal expansion, and may lead to over investments (see small example at the beginning of this section). Considering thermal limits only on tie lines between the considered pair of zones makes sense since the thermal limits of lines between other zones will be embedded in their equivalent physical capacities computations.

The optimization problem presented in (10)-(17) is repeated for every pair of zones connected by a corridor in the reduced network and in the two different directions for each base case snapshot.

Once the optimization problem has been solved for a transfer of power from A to B and for snapshot p, the resulting $A \to B$ maximum flow on the corridor is calculated using the zonal $PTDF$ matrix and the aggregated nodal injections in each zone A and B (equation (18)):

$$F_{A\to B,p} = \sum_z PTDF_{l(AB)}^z INJ'_{z,p} \tag{18}$$

where $PTDF_{l(AB)}^z$ is the element located in row $l(AB)$ and column z of the zonal $PTDF$ matrix; $INJ'_{z,p}$ is the sum of nodal power injections obtained in zone z.

The equivalent zonal network model is used to compute the inter-zonal flows to be coherent with the reactances previously computed. The other inter-zonal flows are calculated in the same way for this set of injections: this is done only if the maximum capacities of tie lines connecting the zones are not violated (only capacities of lines from A to B are considered in this problem). This problem is run again for all the snapshots and every pair of zones in both directions. Finally, for each snapshot, we have several values of the flow over the $A \to B$ inter-zonal corridor: one value from the maximisation of the transfer of power from A to B, and values from the maximisation of transfer of power between other zones where $A \to B$ tie lines capacities are not violated. The $A \to B$ equivalent physical capacity corresponds to the maximum of these $A \to B$ flows over all these values and all the snapshots.

As the flow on each line connecting zones A and B is lower than its thermal limit, the obtained $A \to B$ equivalent physical capacity is lower than the sum of thermal limits of lines connecting A and B:

$$C_{A \to B} \leq \sum\nolimits_{l(ij) \in A \to B \; lines} \overline{F_{l(ij)}} \quad (20)$$

Illustration on a small test case: 9 nodes – 3 zones

In order to illustrate the methodology developed to compute the equivalent capacities of corridors, the same small test case previously employed will be used. The equivalent physical capacities obtained are stated in Table VI.

Table VI **–** Equivalent physical capacities [MW] of the corridors computed using different methods.

Corridor	Considering all network limits	Considering only inter-zonal network limits	Considering only limits of lines in the corridor	Sum of thermal limits of the inter-zonal lines
A-B	293	293	300	300
A-C	182	182	200	200
B-C	100	100	100	100

In the first two cases, there is a risk of under-estimating the equivalent inter-zonal physical capacities, as intra-zonal limits and all inter-zonal limits are considered. The method we implemented corresponds to the third case, where only limits of tie lines connecting the two zones under study are taken into account. We can note that values obtained with the 3 first methods are lower or equal to the sum of thermal limits of inter-zonal lines, which corresponds to an upper bound of the equivalent physical capacities.

6. Task 8.3.6: Grid expansion at nodal level

The expansion at zonal level gives a solution in the form of equivalent physical capacities and reactances between zones for each scenario and time horizon. This is not a directly implementable expansion plan, which needs specific transmission lines with their corresponding end nodes, voltage levels and cable types. Therefore, one of the tasks in the proposed methodology is precisely the obtention of the nodal plan for the two first time horizons (2025 and 2030), for which there is a common zonal expansion plan for all scenarios.

However, the complexities of the power system make it impossible to translate the resulting zonal expansion into an equivalent nodal expansion with identical results for system operation. This task aims as matching them as accurately as possible.

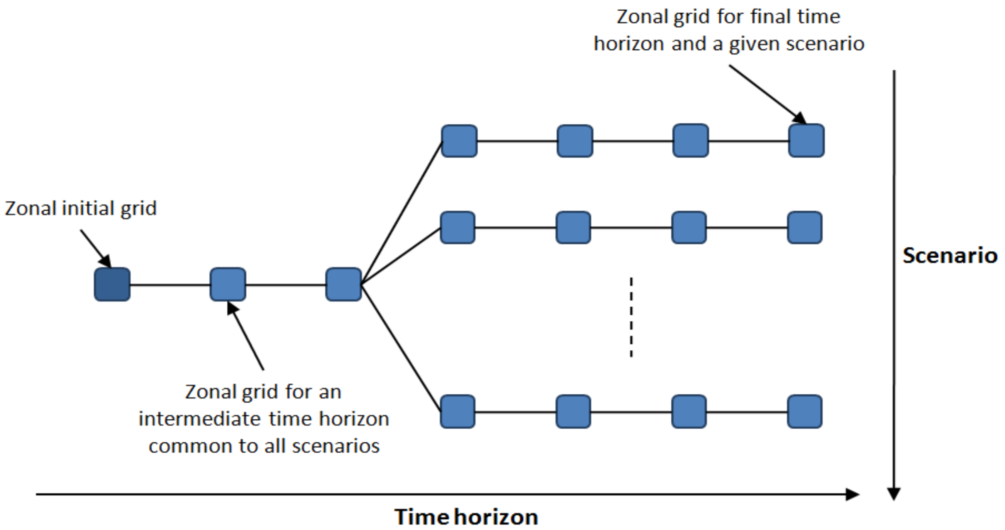

Figure 17. Representation of the expanded network solutions.

We propose to articulate the transcription in two steps:

- First, we identify the most relevant transmission lines that will be considered candidates in the expansion.
- Then, we solve the nodal transmission expansion planning problem to select the optimal lines, taking into account investment and operation cost. This optimization is performed using TEPES (Transmission Expansion Planning for an Electrical System), a model developed by Comillas.

The obtained nodal expansion plans should ensure system reliability (N-1) taking into account all possible flexible devices, while N-1 contingencies were not considered in the former steps.

We detail this two phases in the rest of this section.

6.1. Identification of candidate investments

As in the zonal model, the combinatorial nature of the TEP problem makes it impossible to take into account all possible transmission investments. In the zonal problem, the consideration of the different time horizons gave rise to a dynamic problem. In the case of nodal expansion, the time complexity of the problem is smaller, but the network complexity is much larger as it should consider all specific nodes. The total possible number of lines would be defined by the total number of pairs of nodes in the network and the available cable types. As they are too many to be considered in the optimization problem, it is necessary to focus on the most attractive candidate investments.

We propose to use the candidate proposal mechanism that was presented in (Lumbreras, Ramos, & Sánchez, 2014). This method is based on assessing the potential benefits that are brought by each candidate line. These are approximated as the congestion rent that would be perceived by the transmission line in a hypothetical case where its inclusion did not produce any modifications on system operation. This approximation will generally be higher than the real impact of the line as the nodal prices at the extremes of the transmission line will tend to be closer once a line between them has been installed.

We can use this upper bound on the potential benefits of the transmission line to select the most promising candidates. Subsequently, the optimization will select, from those promising candidates, which ones should be installed in the optimal solution.

The upper bound on congestion rent is calculated as:

$$PB_{ij} = \sum_p DUR_p \left|\sigma_{ip} - \sigma_{jp}\right| \overline{F_{ij}} \tag{18}$$

where:

PB_{ij}: potential benefit of installing a line [M€].

$\overline{F_{ij}}$: rated power of the line [MW],

DUR_p: duration of period p [h]

σ_{ip}: nodal price at node i during period p [h]

An alternative, more accurate calculation of the potential benefit, if a DCLF is used to model system operation can be obtained from the angle difference and the reactance of the circuit:

$$PB_{ij} = \sum_p DUR_p \left(\sigma_{jp} - \sigma_{ip}\right) \frac{(\theta_{ip} - \theta_{jp})}{X_{ij}} \tag{19}$$

where:

θ_{ip}: voltage angle at node i during period p [p.u.]

X_{ij}: rated power of the line [MW],

Once we have calculated the potential benefits, we can identify the promising candidate lines as the ones where the ratio between potential benefits and investment cost is higher than one:

$$BTC_{ijc} = \frac{PB_{ij}}{ic_{ij}} \geq 1 \tag{20}$$

The investment cost of lines is calculated as the product of line cost per km and the distance between its extremes:

$$c_{ij} = CC_c GD_{ij} \tag{21}$$

where:

CC_c: cost of a cable type [M€/km],

GD_{ij}: distance between line extremes [km], which can be adjusted to take into account factors other than geographical distance.

More details on this automatic candidate discovery method can be found in (Lumbreras et al., 2014).

6.2. Grid expansion

Grid expansion must, at the nodal level, select the transmission lines that should be a part of the optimal nodal expansion plan. As explained above, we propose to use the model TEPES (Transmission Expansion Planning for an Electric System), developed by Comillas. A more detailed description of TEPES can be found in reference (Lumbreras & Ramos, 2013).

TEPES is a tool for dynamic tactical transmission expansion planning that decides the new transmission investments (lines, transformers, PSTs) to install in the network. Depending on a user-specified choice, continuous or discrete investments can be used. TEPES is based on stochastic optimization, that is, it finds the expansion plan with the best expected behaviour across the scenarios considered. These scenarios can have different values for demand, renewable generation, fuel or emission costs.

This section presents a stylized version of the formulation of the problem as it is solved in TEPES. For the sake of simplicity, the formulation refers to only one operation situation (snapshot), when actually the model works with average values across scenarios.

First, the base, pre-existing version of TEPES is described. Then, the adjustments that were introduced into the basic model to make it consistent with WP8 are described. TEPES formulates TEP as a Mixed Integer Programming (MIP) problem which minimizes the sum of investment and operation costs, subject to the first and second Kirchhoff's laws and respecting the maximum generation limits and transfer capacities in the system. Power flow calculations are implemented using a DCLF or a transportation model. Losses are approximated, either as a piecewise linear function of the angular difference of the line extremes or as a fixed proportion of the line flow.

6.2.1. Notation

Upper-case symbols denote parameters and sets. Lower-case symbols indicate variables and indices.

Indices

i, j: nodes

p : time period or horizon

l : segments of the piecewise linear approximation of the ohmic losses

N : set of nodes

E, C: set of existing and candidate lines respectively

Parameters

α , β, γ, δ : weights of each component of the objective function [p.u.]

C_{ij} : investment cost of a candidate line [€/MW]

$CENS$: cost of Energy Not Served (ENS) [€/MWh]

CG_i : generation operation cost at a given node i [€/MWh]

D_{pi} : demand at a given node during a period p [MW]

DUR_p: duration of period p [h]

$\overline{F_{ij}}$, $\underline{GP_i}$, $\overline{GP_i}$: limits to transfer capacity and generation respectively [MW]

$\overline{F_{ij}}'$: big-M parameter used to enforce disjunctive constraints [MW]

R_{ij}, X_{ij}: resistance and reactance of each line [p.u.]

S_B: base power [MW]

S_{ijl}, W_{ijl}: slope and width of the segments l of the piecewise linear approximation of line ij losses (computed by the model) [MW] [p.u.]

Variables

x_{ij}: investment decisions where a value of 1 represents the installation of a given candidate line which connects nodes i and j where $(i,j) \in C$ and $x_{ij} \in \{0,1\}$

f_{pij}: flow between nodes i and j through either existing or candidate lines during period p [MW]

l_{pij}: half ohmic losses in each line between nodes i and j during period p [MW]

g_{pi}: generated power at node i during period p [MW]

ens_{pi}: ENS at a given node i during period p [MW]

θ_{pi}: voltage angle at node i during period p [p.u.]

Δw^{+}_{pijl}, Δw^{-}_{pijl}: use of each segment of the piecewise linear approximation of losses [p.u.]

6.2.2. General TEP Model

The objective function adds investment cost, operation cost, generation reliability cost, and transmission reliability cost for the scope of the model.

$$\min InvC + OprC + RelGC + RelNC + PenC \quad (22)$$

Transmission investment cost:

$$InvC = \alpha \sum_{ij \in C} C_{ij} \cdot x_{ij} \quad (23)$$

Generation operation cost:

$$OprC = \beta\left[\sum_{pi} DUR_p \cdot CG_i g_{pi} + \sum_{pi} DUR_p \cdot CENSens_{pi}\right] \quad (24)$$

Generation reliability cost (for each N-1 generation contingency)

$$RelGC = \gamma\left[\sum_{pi} DUR_p \cdot CENSens_{pi}\right] \quad (25)$$

Transmission reliability cost (for each N-1 transmission contingency)

$$RelNC = \delta\left[\sum_{pi} DUR_p \cdot CENSens_{pi}\right] \quad (26)$$

Balance of generation and demand for each node incorporating ohmic losses

$$g_{pi} + \sum_j \left(f_{pji} - f_{pij}\right) + ens_{pi} = D_{pi} + \sum_j \left(l_{pji} - l_{pij}\right), \quad \forall pi \quad (27)$$

TEPES approximates ohmic losses piecewise linearly as a function of the angular difference if the line satisfies a DCLF or as a proportion of the flow if it does not:

$$l_{pij} = S_B \cdot \frac{R_{ij}}{{R_{ij}}^2 + {X_{ij}}^2} \cdot \sum_l S_{ijl}\left(\Delta w^{+}_{pijl} + \Delta w^{-}_{pijl}\right), \quad \forall pi \quad (28)$$

$$l_{pij} = R_{ij} \cdot \sum_l S_{ijl} \cdot \left(\Delta w^+_{pijl} + \Delta w^-_{pijl}\right), \quad \forall pi \tag{29}$$

Second Kirchhoff's law for existing and candidate transmission lines

$$f_{pij} = \left(\theta_{pi} - \theta_{pj}\right)\frac{S_B}{X_{ij}}, \quad \forall pij, ij \in E \tag{30}$$

$$\left|f_{pij} - \left(\theta_{pi} - \theta_{pj}\right)\frac{S_B}{X_{ij}}\right| \leq \overline{F'_{\iota J}}\left(1 - x_{ij}\right), \quad \forall pij, ij \in C \tag{31}$$

where $\overline{F'_{\iota J}}$ is a big-M parameter that is necessary to enforce disjunctive constraints established by running a shortest path problem for each pair of nodes. This is described in (S. Binato et al., 2001).

The second Kirchhoff's law is only met for the candidate lines only if the line is installed, $x_{ij} = 1$. Otherwise, the equation should be relaxed.

Transfer capacity in existing and candidate transmission lines

$$\left|f_{pij}\right| \leq \overline{F_{\iota J}}, \quad \forall pij, ij \in E$$

$$\left|f_{pij}\right| \leq \overline{F_{\iota J}} x_{ij}, \quad \forall pij, ij \in C \tag{32}$$

The relationship between the voltage angle difference at the extremes of the line and the use of a segment of the piecewise linear approximation is calculated in one of two different ways. The first equation is used if the line satisfies a DCLF. The second one is the appropriate one if losses are proportional to the flow:

$$\theta_{pi} - \theta_{pj} = \sum_l \left(\Delta w^+_{pijl} - \Delta w^-_{pijl}\right), \quad \forall pij \tag{33}$$

$$\frac{f_{pij}}{\overline{F_{\iota J}}} = \sum_l \left(\Delta w^+_{pijl} - \Delta w^-_{pijl}\right), \quad \forall pij \tag{34}$$

Maximum and minimum generation constraints:

$$\underline{GP_i} \leq g_{pi} \leq \overline{GP_\iota}, \quad \forall pi$$

$$0 \leq ens_{pi} \leq D_{pi}, \quad \forall pi \tag{35}$$

Bounds on the use of each segment of the piecewise linear losses approximation

$$0 \leq \Delta w^+_{pijl}, \Delta w^-_{pijl} \leq W_{ijl}, \quad \forall pijl \tag{36}$$

This stylized version of the model is not exhaustive. TEPES includes also some other constraints, such as the logical relationships between commitment, start-up and shutdown decisions for subsequent snapshots. Unit commitments are represented using relaxed binary variables. It is possible to establish a specific reserve margin required for the snapshot with maximum demand. Flow exchange constraints between areas or zones can be established. Any flows in excess of these constraints are penalized. In a similar way, maximum and minimum power requirements can be established by each area and technology. These constraints are formulated, in a general way, as:

$$\underline{G}_{pI} - peng^-_{pI} \leq \sum_{i \in I} g_{pi} \leq \bar{G}_{pI} + peng^+_{pI} \tag{37}$$

where

$\underline{G}_{pI}$, $\bar{G}_{pI}$: maximum and minimum limits to the power generated by a set of generators [MW]. The set of generators can be specified by location and technology, for instance.

$peng_{pI}$: penalty applied to an area and technology.

The sum of the penalties is introduced in the objective function.

$$CPen = \sum_{pI} Pnlty^-_{pI} \cdot peng^-_{pI} + \sum_{pI} Pnlty^+_{pI} \cdot peng^+_{pI} \tag{38}$$

Where:

$Pnlty^{-}_{pI}$, $Pnlty^{+}_{pI}$: are the penalties imposed to each deviation from the minimum and maximum energy requirements.

6.2.3. Model Structure

TEPES is built as a two-stage stochastic optimization problem. The first stage determines investments and the second stage describes system operation. Two types of second-stage scenarios are considered. Operation scenarios incorporate a stochastic description of demand and hydro inflows. Reliability scenarios describe contingencies in transmission lines.

TEPES is implemented in GAMS 24.2.3 and is solved with GUROBI. The interface receives data and provides results in Microsoft Excel spreadsheets. In addition, the tool is integrated with Google Earth to provide easy visual inspection of results. The model has been executed in an Intel Xeon X5570 2.93 GHz computer with 12 GB RAM running Microsoft Windows Server 2008 64 bits.

6.2.4. Using TEPES to build a nodal grid architecture consistent with the modular expansion plan

TEPES could be used on the nodal grid directly to find a nodal architecture for the two first horizons. However, the proposed expansion plan would not be necessarily consistent with the modular development plan determined for the full planning scope. Therefore, TEPES is adjusted so that it takes the modular expansion plan as an input, with its resulting inter-zonal capacities, reactances and the zonal injections corresponding to the set of selected snapshots.

We propose to match the increases in inter-zone capacities determined in the zonal expansion at minimum expansion cost.

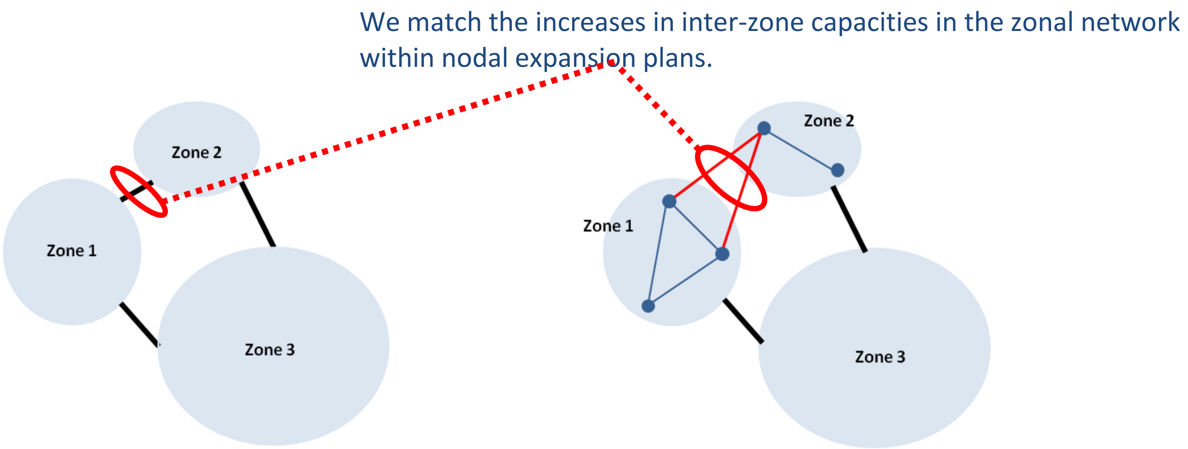

Figure 18. The objective of nodal expansion planning is to match the inter-zone capacities

In order to do this, the basic structure of TEPES has been modified. These modifications are detailed in the rest of this section.

Consistent definition of the objective function

The objective function that guides the zonal expansion is the minimization of the sum of investment cost and a function that penalizes the differences in the injections in the network-constrained model (by node and technology) with respect to the corresponding copperplate injections. We propose to adapt the objective function considered in TEPES to make it consistent with this one. This is achieved by defining the copperplate injections as a constraint for each set of generators by node and injection type (i.e. technology).

$$\underline{G}_{pI} = \bar{G}_{pI} = CPI_{pI} \tag{39}$$

where

CPI_{pI} : copperplate injection for a given node and injection type. The generators belonging to that node and injection type are identified as the set I .

In addition, the parameters that define the additional objectives in the objective function are made equal to zero:

$$\beta = \gamma = \delta = 0 \tag{40}$$

These changes make the objective function be composed of the investment cost of cables and the penalization of the deviation from the power injections in the copperplate model (we use the same costs than the ones from DCOPF).

These costs are calculated over the same snapshots selected for the zonal expansion planning (see D8.4.a "Enhanced methodology to define the optimal modular plan").

Enforcement of modular expansion plan

The nodal grid expansion must approximate as closely as possible the final capacities determined in the zonal expansion. The nodal expansion plan is composed of two types of transmission lines: the transmission lines that link two different zones and the ones that belong inside a zone. Both of them are considered by TEPES, as it deals with the nodal grid. The zonal plan establishes the final inter-zonal capacities. They are enforced by introducing the constraints:

$$\sum_{\substack{i\in a \\ j\in b}} \overline{F_{ij}} x_{ij} \geq Cap_{ab} \ , \ \forall ab/a \neq b \tag{41}$$

where

ab: pairs of zones. The nodes belonging to a given zone are denoted as $i \in a, j \in b$.

Cap_{ab}: final inter-zonal capacity determined in the modular expansion plan for each pair of zones.

Meeting these minimum inter-zonal capacity constraints is a necessary condition to follow the outcome of the zonal plan. As investment cost is weighted in the objective function, these will be met at minimum cost.

The zonal plan does not give any information about internal reinforcements. They are left to the discretion of the nodal expansion entirely and will be chosen to minimize total costs.

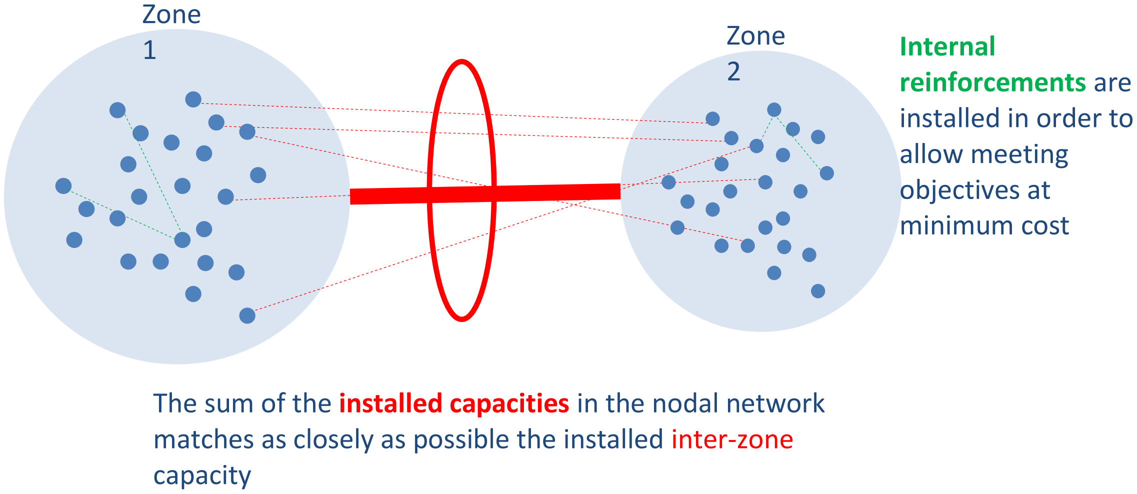

Figure 19. Representation of the reduced network

Consideration of different technologies and cable types

TEPES can consider several voltage levels and transmission technologies directly. We use them to define the following types of transmission investment:

- HVAC transmission lines abide Kirchhoff's First and Second Laws.
- HVDC transmission lines abide only Kirchhoff's First Law. In the model, the constraints that enforce the Second Law only applies if the transmission line is labelled as an AC line.
- If an HVAC transmission line of higher voltage than the current voltage of the nodes is installed, the cost of a transformer to elevate the voltage at both ends of the line is taken into account.
- If an HVDC line is installed, the model includes also the cost of the converter stations at both ends of the line.
- If a PST is installed, the model assumes that line capacity of the line stays the same and Kirchhoff's Second Law is relaxed. This is considered a sufficiently good approximation of the PST behaviour for the purposes of transmission expansion.

Reliability considerations

TEPES can consider reliability as a partial objective. This is carried out by including stochastic scenarios that describe either generation or transmission contingencies. However, given the size of the nodal network, the consideration of the full set of contingencies is not possible. Therefore, we propose the following:

- Particularly important elements, such as HVDC lines, are considered explicitly.
- The reliability of other transmission lines is considered implicitly by means of imposing redundancy constraints to the transmission lines added to the grid. This redundancy is established to limit the capacity that is lost if one line fails, and follows the heuristic defined in reference (McCalley, Aliprantis, D., Dobson, A., Li, & Villegas, 2013).

This heuristic assumes that there is a pre-existing line of capacity C_0.The expansion plan will add n new lines of capacity C. Because of reliability reasons, the flow is limited to a maximum proportion of capacity, p.

$$pnC + pC_0 \leq (n-1)C + C_0 \qquad (42)$$

$$\frac{C}{C_0} \leq \frac{(1-p)}{(np-n+1)} \tag{43}$$

According to reference (McCalley et al., 2013), investment economics can be attractive if total new capacity is significant relative to the existing capacity. Operational economics can be attractive if we can use a significant percentage of the total capacity.

- $n = 1$ or $n = 2$ does not give a good ratio for $C/_{C_0}$, unless p is very small.
- $n = 3$ enables to build lines with 100% of the existing capacity while using 75% of the total capacity.
- $n > 3$ can be used for a higher proportion.

We can use the table below for determining the most appropriate overlays depending on the proportion of flow that we consider.

Table VII **–** Maximum proportion between the capacity of the reinforcements and the original one depending on the proportion of flow allowed and the number of corridors added.

p	n	Maximum $C/_{C_0}$
0,7	1	0,429
0,7	2	0,75
0,7	3	3
0,75	1	0,33
0,75	2	0,5
0,75	3	1
0,8	1	0,25
0,8	2	0,33
0,8	3	0,5
0,9	1	0,111
0,9	2	0,125
0,9	3	0,143

This heuristic is implemented in TEPES in order to determine the most suitable reinforcements for existing corridors.

Figure 20 shows the results obtained with TEPES. It returns a map with the proposed network expansions.

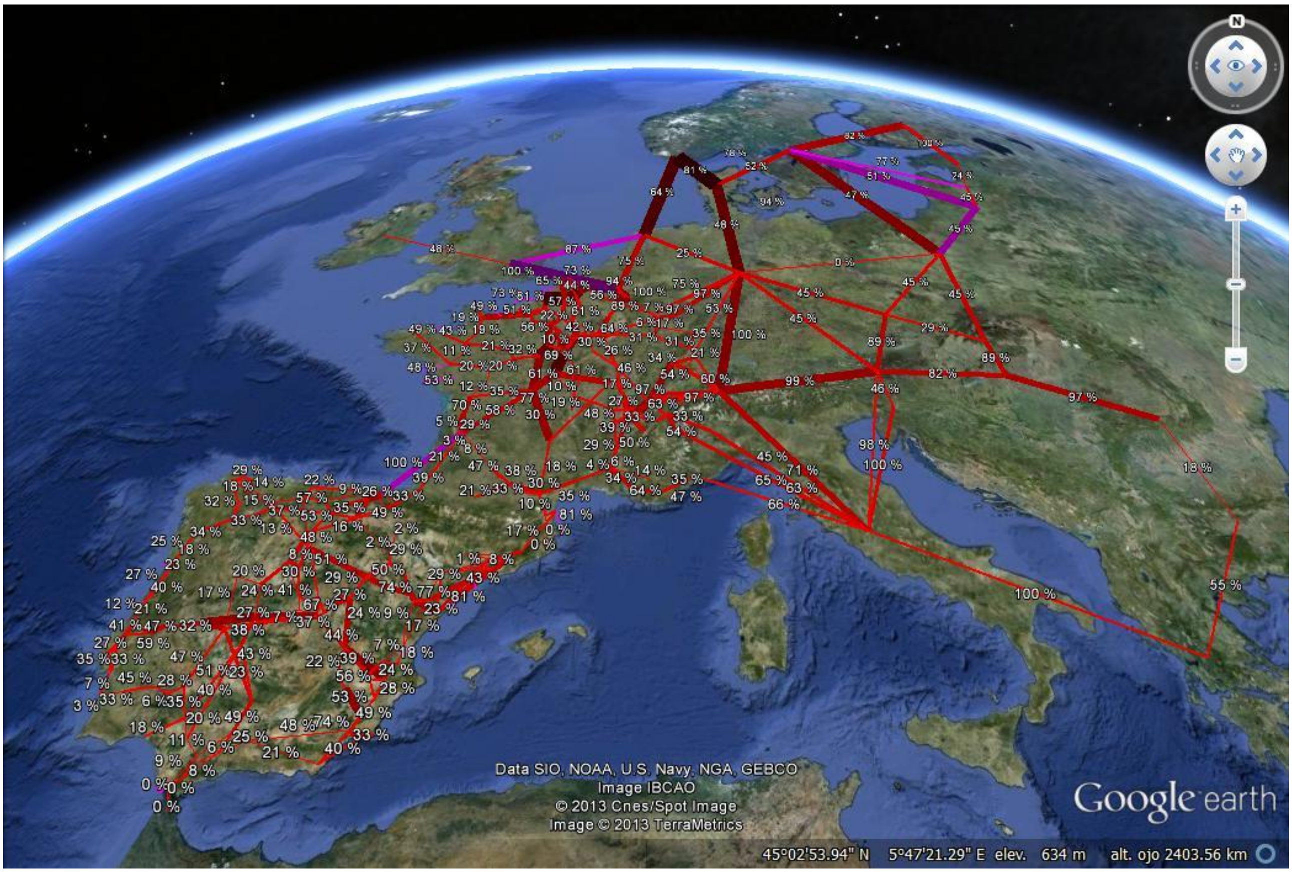

Figure 20. Representation of an example expansion plan obtained with TEPES

7. References

Akbari, T., Zolfaghari, S., & Kazemi, A. (2009). Multi-stage stochastic transmission expansion planning under load uncertainty using benders decomposition. *International Review of Electrical Engineering, 4*(5), 976-984.

Alseddiqui, J., & Thomas, R. J. (2006). Transmission expansion planning using multi-objective optimization. *Power Engineering Society General Meeting, 2006. IEEE,* pp. 8 pp.

Alvarez, J., Ponnambalam, K., & Quintana, V. H. (2006). Transmission expansion under risk using stochastic programming. *Probabilistic Methods Applied to Power Systems, 2006. PMAPS 2006. International Conference on,* pp. 1-7.

Bahiense, L., Oliveira, G. C., Pereira, M., & Granville, S. (2001). A mixed integer disjunctive model for transmission network expansion. *Power Systems, IEEE Transactions on, 16*(3), 560-565.

Bennon, R. J., Juves, J. A., & Meliopoulos, A. P. (1982). Use of sensitivity analysis in automated transmission planning. *Power Apparatus and Systems, IEEE Transactions on, PAS-101*(1), 53-59.

Binato, S., de Oliveira, G. C., & de Araujo, J. L. (2001). A greedy randomized adaptive search procedure for transmission expansion planning. *Power Systems, IEEE Transactions on, 16*(2), 247-253.

Binato, S., Pereira, M. V. F., & Granville, S. (2001). A new benders decomposition approach to solve power transmission network design problems. *IEEE Transactions on Power Systems, 16*(2), 235.

Blumsack, S., Hines, P., Patel, M., Barrows, C., & Cotilla Sanchez, E. (2009). Defining power network zones from measures of electrical distance. *Power & Energy Society General Meeting, 2009. PES '09. IEEE,* pp. 1-8.

Braga, A. S. D., & Saraiva, J. T. (2005). A multiyear dynamic approach for transmission expansion planning and long-term marginal costs computation. *Power Systems, IEEE Transactions on, 20*(3), 1631-1639.

Bulent Tor, O., Nezih Guven, A., & Shahidehpour, M. (2008). Congestion-driven transmission planning considering the impact of generator expansion. *IEEE Transactions on Power Systems, 23*(2), 781-789.

Cagigas, C., & Madrigal, M. (2003). Centralized vs. competitive transmission expansion planning: The need for new tools. *Power Engineering Society General Meeting, 2003, IEEE, , 2.* pp. 1017 Vol. 2.

Carrión, M., Arroyo, J. M., & Alguacil, N. (2007). Vulnerability-constrained transmission expansion planning: A stochastic programming approach. *IEEE Transactions on Power Systems, 22*(4), 1436-1445.

Chanda, R. S., & Bhattacharjee, P. K. (1994). Application of computer software in transmission expansion planning using variable load structure. *Electric Power Systems Research, 31*(1), 13-20.

Costeira, M., & Saraiva, J. T. Discrete evolutionary particle swarm optimization for multiyear transmission expansion planning. *17th Power Systems Computation Conference,* Stockholm, Sweden.

Cotilla-Sanchez, E., Hines, P. D. H., Barrows, C., Blumsack, S., & Patel, M. (2013). Multi-attribute partitioning of power networks based on electrical distance. *Power Systems, IEEE Transactions on, 28*(4), 4979-4987.

Da Silva, A. M. L., Rezende, L. S., Manso, L. A. F., & Anders, G. J. (2010). Transmission expansion planning: A discussion on reliability and "N−1" security criteria. *Probabilistic Methods Applied to Power Systems (PMAPS), 2010 IEEE 11th International Conference on,* pp. 244-251.

Da Silva, E. L., Ortiz, J. M. A., De Oliveira, G. C., & Binato, S. (2001). Transmission network expansion planning under a tabu search approach. *Power Systems, IEEE Transactions on, 16*(1; a metaheuristic proposed in 1989 to be applied to combinatorial problems. To assess the potential of our approach we test it with two cases of transmission network expansion planning. The results obtained), 62-68.

Dahman, S. R., Morrow, D. J., Tynes, K., & Weber, J. D. (2008). Advanced sensitivity analysis for long-range transmission expansion planning. *Hawaii International Conference on System Sciences, Proceedings of the 41st Annual,* pp. 166-166.

De la Torre, S., Conejo, A. J., & Contreras, J. (2008). Transmission expansion planning in electricity markets. *Power Systems, IEEE Transactions on, 23*(1), 238-248.

Dechamps, C., & Jamoulle, E. (1980). Interactive computer program for planning the expansion of meshed transmission networks. *International Journal of Electrical Power & Energy Systems, 2*(2), 103-108.

Di Shi, & Tylavsky, D. J. (2012). An improved bus aggregation technique for generating network equivalents. *Power and Energy Society General Meeting, 2012 IEEE,* pp. 1-8.

Dodu, J. C., Ludot, J. P., & Pouget, J. (1969). Sur le regroupement optimal des sommets dans un réseau électrique. *RAIRO, Recherche opérationnelle,* vol. 1, pp. 17-37.

Dusonchet, Y. P., & El-Abiad, A. (1973). Transmission planning using discrete dynamic optimizing. *Power Apparatus and Systems, IEEE Transactions on, PAS-92*(4), 1358-1371.

Ekwue, A. O., & Cory, B. J. (1984). Transmission system expansion planning by interactive methods. *Power Apparatus and Systems, IEEE Transactions on, PAS-103*(7), 1583-1591.

El-Keib, A. A., Jaeseok Choi, & Trungtinh Tran. (2006). Transmission expansion planning considering ambiguities using fuzzy modeling. *Power Systems Conference and Exposition, 2006. PSCE '06. 2006 IEEE PES,* pp. 207-215.

Escobar , A. (2002). *Planeamiento dinámico de la expansión de sistemas de transmisión usando algoritmos combinatoriales.* Unpublished

Feintuch, P. (1983). Power system expansion planning at EDF. *International Journal of Electrical Power & Energy Systems, 5*(2), 115-120.

Gajbhiye, R. K., Naik, D., Dambhare, S., & Soman, S. A. (2008). An expert system approach for multi-year short-term transmission system expansion planning: An indian experience. *Power Systems, IEEE Transactions on, 23*(1), 226-237.

Gallego, R. A., Alves, A. B., Monticelli, A., & Romero, R. (1997). Parallel simulated annealing applied to long term transmission network expansion planning. Power Systems, IEEE Transactions on, 12(1), 181-188.

Garcés, A., & Molinas, M. (2009). Cluster interconnection of offshore wind farms using direct AC high frequency links.

Garver, L. L. (1970). Transmission network estimation using linear programming. *Power Apparatus and Systems, IEEE Transactions on, PAS-89*(7), 1688-1697.

Garzillo, A., Cazzol, M. V., L'Abbate, A., Migliavacca, G., Mansoldox, A., Riverax, A., et al. (2010). Offshore grids in europe: The strategy of ireland for 2020 and beyond. *AC and DC Power Transmission, 2010. ACDC. 9th IET International Conference on,* pp. 1-7.

Gorenstin, B. G., Campodonico, N. M., Costa, J. P., & Pereira, M. V. F. (1993). Power system expansion planning under uncertainty. *IEEE Transactions on Power Systems, 8*(1), 129-136.

Haffner, S., Monticelli, A., Garcia, A., Mantovani, J., & Romero, R. (2000). Branch and bound algorithm for transmission system expansion planning using a transportation model. *Generation, Transmission and Distribution, IEE Proceedings-, 147*(3), 149-156.

Haixia Wang, Rao Liu, Weidong Li, & Caihong Zhao. (2009). Power flow tracing with consideration of the electrical distance. *Power and Energy Engineering Conference, 2009. APPEEC 2009. Asia-Pacific,* pp. 1-4.

Hamon, C., Shayesteh, E., Amelin, M., & Söder, L. (2014). Two partitioning methods for multi-area studies in large power systems. *International Transactions on Electrical Energy Systems,* , n/a-n/a.

Hartigan, J. A., & Wong, M. A. (1979). Algorithm AS 136: A K-means clustering algorithm. *Applied Statistics, 28*(1), 100-108.

Hesamzadeh, M. R., Hosseinzadeh, N., & Wolfs, P. J. (2008). Economic assessment of transmission expansion projects in competitive electricity markets - an analytical review. *Universities Power Engineering Conference, 2008. UPEC 2008. 43rd International,* pp. 1-10.

Infanger, G. (1992). Monte carlo (importance) sampling within a benders decomposition algorithm for stochastic linear programs. *Annals of Operations Research, 39*(1-4), 69-95.

J. O. G. Tande, M. Korpås, L. Warland, K. Uhlen, F. Van Hulle. (2008). *Impact of TradeWind offshore wind power capacity scenarios on power flows in the european HV network* 7th International Workshop on Large Scale Integration of Wind Power and on Transmission Networks for Offshore Wind Farms. Joong-Rin Shin, & Young-Moon Park. (1993). Optimal long-term transmission planning by expert system approach. *TENCON '93. Proceedings. Computer, Communication, Control and Power Engineering.1993 IEEE Region 10 Conference on,* (0) pp. 713-717 vol.2.

Jun Hua Zhao, Foster, J., Zhao Yang Dong, & Kit Po Wong. (2011). Flexible transmission network planning considering distributed generation impacts. *Power Systems, IEEE Transactions on, 26*(3), 1434-1443.

Kagan, N., & Adams, R. N. (1990). Application of benders' decomposition technique to the distribution planning problem. *PSCC. Proceedings of the Tenth Power Systems Computation Conference,*

Kaltenbach, J. C., Peschon, J., & Gehrig, E. H. (1970). A mathematical optimization technique for the expansion of electric power transmission systems. *Power Apparatus and Systems, IEEE Transactions on, PAS-89*(1), 113-119.

Latorre, G., Cruz, R. D., Areiza, J. M., & Villegas, A. (2003). Classification of publications and models on transmission expansion planning. *Power Systems, IEEE Transactions on, 18*(2), 938-946.

Latorre, G., Ramos, A., Pérez-Arriaga, J. I., Alonso, J. F., & Sáiz, A. (1991). PERLA: A static model for long-term transmission planning. modeling options and suitability analysis. *Proc. 2nd Spanish-Portuguese Conf. Elect. Eng.*

Latorre, J. M., Cerisola, S., & Ramos, A. (2007). Clustering algorithms for scenario tree generation: Application to natural hydro inflows. *European Journal of Operational Research, 181*(3), 1339-1353.

Latorre-Bayona, G., & Perez-Arriaga, I. J. (1994). CHOPIN, a heuristic model for long term transmission expansion planning. *Power Systems, IEEE Transactions on, 9*(4), 1886-1894.

Lee, C. W., Ng, S. K. K., & Zhong, J. (2007). Portfolio optimization in transmission investment in deregulated market. *Power Engineering Society General Meeting, 2007. IEEE,* pp. 1-8.

Lee, S. T. Y., Hicks, K. L., & Hnyilicza, E. (1974). Transmission expansion by branch-and-bound integer programming with optimal cost - capacity curves. *Power Apparatus and Systems, IEEE Transactions on, PAS-93*(5), 1390-1400.

Levi, V. A., & Calovic, M. S. (1991). A new decomposition based method for optimal expansion planning of large transmission networks. *Power Systems, IEEE Transactions on, 6*(3), 937-943.

Lu, M., Dong, Z. Y., & Saha, T. K. (2005). Transmission expansion planning flexibility. *Power Engineering Conference, 2005. IPEC 2005. the 7th International,* pp. 893-898 Vol. 2.

Lumbreras, S., & Ramos, A. (2013). Transmission expansion planning using an efficient version of benders' decomposition. A case study. *PowerTech (POWERTECH), 2013 IEEE Grenoble,* pp. 1-7.

Lumbreras, S., Ramos, A., & Sánchez, P. (2014). Automatic selection of candidate investments for transmission expansion planning. *International Journal of Electrical Power & Energy Systems, 59*(0), 130-140.

Maghouli, P., Hosseini, S. H., Buygi, M. O., & Shahidehpour, M. (2009). A multi-objective framework for transmission expansion planning in deregulated environments. *Power Systems, IEEE Transactions on, 24*(2), 1051-1061.

Maghouli, P., Hosseini, S. H., Buygi, M. O., & Shahidehpour, M. (2011). A scenario-based multi-objective model for multi-stage transmission expansion planning. *Power Systems, IEEE Transactions on, 26*(1), 470-478.

Marin, A., & Salmeron, J. (1998). Electric capacity expansion under uncertain demand: Decomposition approaches. *IEEE Transactions on Power Systems, 13*(2), 333-339.

McCalley, J. D., Aliprantis, D., Dobson, A., Li, Y., & Villegas, H. (2013). *High capacity interregional transmission system design*Report for RTE.

Meliopoulos, A. P., Webb, R. P., Bennon, R. J., & Juves, J. A. (1982). Optimal long range transmission planning with AC load flow. *Power Apparatus and Systems, IEEE Transactions on, PAS-101*(10), 4156-4163.

Meza, J. L. C., Yildirim, M. B., & Masud, A. S. M. (2007). A model for the multiperiod multiobjective power generation expansion problem. *Power Systems, IEEE Transactions on, 22*(2), 871-878.

Miranda, V., & Proenca, L. M. (1998a). Probabilistic choice vs. risk analysis-conflicts and synthesis in power system planning. *Power Systems, IEEE Transactions on, 13*(3), 1038-1043.

Miranda, V., & Proenca, L. M. (1998b). Why risk analysis outperforms probabilistic choice as the effective decision support paradigm for power system planning. *Power Systems, IEEE Transactions on, 13*(2), 643-648.

Moeini-Aghtaie, M., Abbaspour, A., & Fotuhi-Firuzabad, M. (2012a). Incorporating large-scale distant wind farms in probabilistic transmission expansion Planning—Part I: Theory and algorithm. *Power Systems, IEEE Transactions on, PP*(99), 1-1.

Moeini-Aghtaie, M., Abbaspour, A., & Fotuhi-Firuzabad, M. (2012b). Incorporating large-scale distant wind farms in probabilistic transmission expansion Planning—Part II: Case studies. *Power Systems, IEEE Transactions on, PP*(99), 1-1.

Moghaddam, M. P., Abdi, H., & Javidi, M. H. (2006). Transmission expansion planning in competitive electricity markets using AC OPF. *Power Systems Conference and Exposition, 2006. PSCE '06. 2006 IEEE PES,* pp. 1507-1512.

Na, S., Xumin, L., & Yong, G. (2010). Research on k-means clustering algorithm and improved k-means clustering algorithm. *2010 Third International Symposium Conf. on Intelligent Information Technology and Security Informatics (IITSI),* pp. 63-67.

Oh, H., & Short, W. (2009). Optimal expansion planning for the deployment of wind energy. *Journal of Energy Engineering, 135*(3), 83-88.

Oliveira, G. C., Binato, S., & Pereira, M. V. F. (2007). Value-based transmission expansion planning of hydrothermal systems under uncertainty. *Power Systems, IEEE Transactions on, 22*(4), 1429-1435.

Oliveira, G. C., Costa, A. P. C., & Binato, S. (1995). Large scale transmission network planning using optimization and heuristic techniques. *Power Systems, IEEE Transactions on, 10*(4), 1828-1834.

Olmos, L., Rivier, M., & Cabezudo, D. (2013). An analysis of the marginal value of electricity transmission lines in the dispatch: Possible applications. *Power Systems, IEEE Transactions on, 28*(3), 2737-2748.

Peco, J., Sanchez-Ubeda, E. F., & Gomez, T. (1999). Enhancing optimal transmission or subtransmission planning by using decision trees. *Electric Power Engineering, 1999. PowerTech Budapest 99. International Conference on,* pp. 175.

Pereira, M. V. F., Pinto, L. M. V. G., Cunha, S. H. F., & Oliveira, G. C. (1985). A decomposition approach to automated generation/transmission expansion planning. *IEEE Transactions on Power Apparatus and Systems, PAS-104*(11), 3074-3083.

REE, "The Spanish Electricity System Report 2012", 2013. Available at: http://www.ree.es/en/publications/spanish-electrical-system/spanish-electricity-system-report-2012

Rezende, L. S., Leite da Silva, A. M., & Honorio, L. M. (2009). Artificial immune systems and differential evolution based approaches applied to multi-stage transmission expansion planning. *Intelligent System Applications to Power Systems, 2009. ISAP '09. 15th International Conference on,* pp. 1-6.

RTE, "Actualisation du Bilan Prévisionnel de l'équilibre offre-demande d'électricité en France", 2013. Available at: http://www.rte-france.com/sites/default/files/bilan_actualisation_2013_v2.pdf

Risheng Fang, & Hill, D. J. (2003). A new strategy for transmission expansion in competitive electricity markets. *Power Systems, IEEE Transactions on, 18*(1), 374-380.

Romero, R., Gallego, R. A., & Monticelli, A. (1995). Transmission system expansion planning by simulated annealing. *Power Industry Computer Application Conference, 1995. Conference Proceedings., 1995 IEEE,* pp. 278-283.

Romero, R., & Monticelli, A. (1994a). A hierarchical decomposition approach for transmission network expansion planning. *Power Systems, IEEE Transactions on, 9*(1), 373-380.

Romero, R., & Monticelli, A. (1994b). A zero-one implicit enumeration method for optimizing investments. *Power Systems, IEEE Transactions on, 9*(3), 1385-1391.

Romero, R., Rider, M. J., & Silva, I. d. J. (2007). A metaheuristic to solve the transmission expansion planning. *Power Systems, IEEE Transactions on, 22*(4), 2289-2291.

Rudnick, H., Palma, R., Cura, E., & Silva, C. (1996). Economically adapted transmission systems in open access schemes-application of genetic algorithms. *Power Systems, IEEE Transactions on, 11*(3), 1427-1440.

Seifu, A., Salon, S., & List, G. (1989). Optimization of transmission line planning including security constraints. *Power Systems, IEEE Transactions on, 4*(4), 1507-1513.

Serna, C., Duran, J., & Camargo, A. (1978). A model for expansion planning of transmission systems A practical application example. *Power Apparatus and Systems, IEEE Transactions on, PAS-97*(2), 610-615.

Sharifnia, A., & Aashtiani, H. Z. (1985). Transmission network planning: A method for synthesis of minimum-cost secure networks. *Power Apparatus and Systems, IEEE Transactions on, PAS-104*(8), 2025-2034. Siddiqi, S. N., & Baughman, M. L. (1995). Value-based transmission planning and the effects of network models. *Power Systems, IEEE Transactions on, 10*(4), 1835-1842.

Silva, I. J., Rider, M. J., Romero, R., & Murari, C. A. (2006). Genetic algorithm of chu and beasley for static and multistage transmission expansion planning. *Power Engineering Society General Meeting, 2006. IEEE,* pp. 7 pp.

Sum-Im, T., Taylor, G. A., Irving, M. R., & Song, Y. H. (2009). Differential evolution algorithm for static and multistage transmission expansion planning. *Generation, Transmission & Distribution, IET, 3*(4), 365-384.

Teive, R. C. G., Silva, E. L., & Fonseca, L. G. S. (1998). A cooperative expert system for transmission expansion planning of electrical power systems. *Power Systems, IEEE Transactions on, 13*(2), 636-642.

Tsamasphyrou, P., Renaud, A., & Carpentier, P. (1999). *Transmission network planning: An efficient benders decomposition scheme*. *Power Systems Computation Conference (PSCC),* Trondheim (Norway).

Vasquez, P., Styczynski, Z. A., & Vargas, A. (2008). Flexible decision making-based framework for coping with risks existing in transmission expansion plans. *Transmission and Distribution Conference and Exposition: Latin America, 2008 IEEE/PES,* pp. 1-9.

Villasana, R., Garver, L. L., & Salon, S. J. (1985). Transmission network planning using linear programming. *Power Apparatus and Systems, IEEE Transactions on, PAS-104*(2), 349-356.

Vinasco, G., Rider, M. J., & Romero, R. (2011). A strategy to solve the multistage transmission expansion planning problem. *Power Systems, IEEE Transactions on, 26*(4), 2574-2576.

Xie, M., Zhong, J., & Wu, F. F. (2007). Multiyear transmission expansion planning using ordinal optimization. *IEEE Transactions on Power Systems, 22*(4), 1420-1428.

Xu, Z., Dong, Z. Y., & Wong, K. P. (2006). Transmission planning in a deregulated environment. *Generation, Transmission and Distribution, IEE Proceedings-, 153*(3), 326-334.

Yoshimoto, K., Yasuda, K., & Yokoyama, R. (1995). Transmission expansion planning using neuro-computing hybridized with genetic algorithm. *Evolutionary Computation, 1995., IEEE International Conference on, , 1.* pp. 126.

Youssef, H. K., & Hackam, R. (1989). New transmission planning model. *Power Systems, IEEE Transactions on, 4*(1), 9-18.

Zhao Xu, Zhao Yang Dong, & Kit Po Wong. (2006). A hybrid planning method for transmission networks in a deregulated environment. *Power Systems, IEEE Transactions on, 21*(2), 925-932.

8. Appendix A: Existing TEP approaches

This section describes the main TEP approaches existing both in literature and in current practice. As a result of its importance, this problem has been studied extensively in both practical and academic contexts (G. Latorre, Cruz, Areiza, & Villegas, 2003). This has resulted in the application of a wide array of solution methodologies with varying levels of technical soundness and applicability to large-scale cases. These techniques can be classified in two main families:

Automatic methodologies rely on an agreed set of optimization criteria (for instance, the ones defined in WP2 or WP6) or expansion rules with no further requirement for human intervention. Within automatic methodologies, two types of methods should be distinguished:

- **Optimization methods** provide with the best possible (or quasi-optimal) expansion plans according to the established criteria.
- **Intelligent search** based on heuristic rules applies some pre-determined actions in order to improve the existing network. This approach cannot guarantee optimality.

Iterative search techniques seek a suitable expansion plan by recurrently combining information from two different modules:

- A planning module (or network module, according to the terminology adopted in e-Highway2050) proposes investments using available technical and economic power system information. Proposals are usually selected by planners who have expert knowledge on the system, such as the relevant TSO.
- An operation module (market module) recalculates the operation of the system and computes technical-economic indicators to be subsequently input into the planning module. This operation model may or not include the specific analysis of extreme events or reliability scenarios. Indicators produced in the operation module should be relevant for the computation of the required network reinforcements and may include the set of potential investments to be analysed by the planning module at a later stage.

In addition, the selected methodology must be able to accommodate the modelling characteristics that have been regarded as relevant by the planner, such as the technical expansion options available or the appropriate description of uncertainty.

The potential techniques offer different trade-offs in terms of optimality of the expansion plan and ability to cope with large systems or high levels of modelling detail. This document reviews their main characteristics as well as the cases where their application would be most suitable. This report is organized as follows. First, automatic methodologies are described, classifying them into optimization methods and intelligent search techniques. Then, iterative search methods are discussed. Finally, some considerations on the treatment of different technological options and the incorporation of uncertainty are presented.

8.1. Automatic transmission expansion planning approaches

Automatic approaches are able to provide with an optimal or quasi-optimal expansion plans without any need for intervention from the planner once the problem has been defined. This definition includes system data and the agreed set of rules or optimization criteria. This results in **objectively defined** expansion plans that are, in the case of classical optimization, **optimal**. This provides a significant advantage if the system under study is large or the available expertise on the system is limited so that iterative approaches could result in considerably suboptimal solutions. This automatic approach can be especially useful in the case of large-scale systems where system-wide expert knowledge is limited, such as the European case.

The most relevant solution techniques within the automatic methodologies context are presented in this section.

8.1.1. Optimization of the expansion of the grid

Optimization methods use a **dedicated tool** to propose the best possible expansion plan according to a set of agreed criteria. This typically involves **maximizing total welfare** or, equivalently, minimizing total system costs.

This methodology is suitable to deal with the **medium and long-term planning of systems of all sizes.** However, **system operation must usually be described in a simplified way** in order to keep the problem computationally tractable. For instance, technical constraints such as voltage limitations, dynamic stability conditions or maximum short circuit currents are generally not included in the optimization model.

This implies that **the feasibility of the optimal plan should be assessed** at a subsequent stage using a separate grid analysis tool. If the infeasibilities detected are local and limited, changes to the expansion plan can be proposed, probably in an automated way. Otherwise, it is possible to use the identified problems to define new constraints that will be added to the optimization problem. In the latter case, the process of search for the optimal network architecture would not be fully automatic.

Several alternative techniques can be identified within the optimization context.

Classical methods

Classical methods are the only ones able to provide an **optimality guarantee** on the solution. This is, it is possible to use the method to find a solution that is either optimal or within a tolerance distance from the optimal one. Different techniques are available.

Linear programming applies very efficient algorithms to solve the problem in affordable times. This option has been widely used in the academic literature (Chanda & Bhattacharjee, 1994; Feintuch, 1983; Garver, 1970; Meza, Yildirim, & Masud, 2007; Villasana, Garver, & Salon, 1985). This method requires the description of the system to be linear, which implies using either a transportation model or a DCPF for system operation (no consideration of reactive power and voltage constraints, neither of the true nonlinear function of network losses) and ignoring the discrete nature of network investments. However, using a simplified model has the advantage of being able to cope with very large systems and number of scenarios.

Quadratic programming is generally used to add a quadratic approximation of losses to a linear system operation model (J. O. G. Tande, M. Korpås, L. Warland, K. Uhlen, F. Van Hulle, 2008).

Mixed Integer Programming (MIP) and Mixed Integer Quadratic Programming (MIQP) acknowledge the integrality of network investments (i.e., a corridor can be installed or not, but there are no intermediate stages in between). Current powerful algorithms can be applied to solve the problem. This is also a very popular choice in the academic literature, (Alvarez, Ponnambalam, & Quintana, 2006; Bahiense, Oliveira, Pereira, & Granville, 2001; S. Binato, Pereira, & Granville, 2001; Bulent Tor, Nezih Guven, & Shahidehpour, 2008; Carrión, Arroyo, & Alguacil, 2007; de la Torre, Conejo, & Contreras, 2008; Garcés & Molinas, 2009; Garzillo et al., 2010; Gorenstin, Campodonico, Costa, & Pereira, 1993; Haffner, Monticelli, Garcia, Mantovani, & Romero, 2000; Infanger, 1992; Kagan & Adams, 1990; G. Latorre, Ramos, Pérez-Arriaga, Alonso, & Sáiz, 1991; C. W. Lee, Ng, & Zhong, 2007; S. T. Y. Lee, Hicks, & Hnyilicza, 1974; Oh & Short, 2009; Oliveira, Costa, & Binato, 1995; Oliveira, Binato, & Pereira, 2007; Pereira, Pinto, Cunha, & Oliveira, 1985; Romero & Monticelli, 1994a; Romero & Monticelli, 1994b; Seifu, Salon, & List, 1989; Sharifnia & Aashtiani, 1985; Tsamasphyrou, Renaud, & Carpentier, 1999; Vinasco, Rider, & Romero, 2011).

If a linear operation model is not deemed appropriate, an ACPF can be implemented using **Nonlinear Programming** (NLP) or **Mixed Integer Nonlinear Programming** (MINLP) (Alseddiqui & Thomas, 2006; Marin & Salmeron, 1998; Meliopoulos, Webb, Bennon, & Juves, 1982; Moghaddam, Abdi, & Javidi, 2006; Siddiqi & Baughman, 1995; Youssef & Hackam, 1989). However, implementations of these methods usually require very long computation times and can be unable to deal with large problem sizes due to the lack of powerful nonlinear optimization solvers.

Stochastic decomposition techniques, such as Benders' decomposition, can be interestingly applied in order to efficiently deal with large sets of uncertain scenarios (Akbari, Zolfaghari, & Kazemi, 2009; S. Binato et al., 2001; Bulent Tor et al., 2008; Haffner et al., 2000; Infanger, 1992; Kagan & Adams, 1990; G. Latorre et al., 1991; Latorre-Bayona & Perez-Arriaga, 1994; Marin & Salmeron, 1998; Oliveira et al., 1995; Pereira et al., 1985; Romero & Monticelli, 1994b; Siddiqi & Baughman, 1995; Tsamasphyrou et al., 1999).

Non-classical optimization methods

Non-classical methods are generally able to deal with **large problem sizes** and **varying levels of modeling detail** in **affordable computation times**. The methods guarantee that the obtained expansion plan will progressively approach the optimal solution. However, bounds on the distance to the optimal solution cannot generally be provided.

The most commonly used non-classical methods include Genetic Algorithms (A. M. L. da Silva, Rezende, Manso, & Anders, 2010; Maghouli, Hosseini, Buygi, & Shahidehpour, 2009; Miranda & Proenca, 1998b; Moeini-Aghtaie, Abbaspour, & Fotuhi-Firuzabad, 2012a; Moeini-Aghtaie, Abbaspour, & Fotuhi-Firuzabad, 2012b; Peco, Sanchez-Ubeda, & Gomez, 1999; Rudnick, Palma, Cura, & Silva, 1996; Silva, Rider, Romero, & Murari, 2006; Xu, Dong, & Wong, 2006; Yoshimoto, Yasuda, & Yokoyama, 1995), (which emulate the dynamics of natural selection), Simulated Annealing (which mirrors the thermodynamical process of a slowly cooling system) (Braga & Saraiva, 2005; Braga & Saraiva, 2005; Gallego, Alves, Monticelli, & Romero, 1997; Romero, Gallego, & Monticelli, 1995) or Swarm Intelligence (Costeira & Saraiva, ; Jun Hua Zhao, Foster, Zhao Yang Dong, & Kit Po Wong, 2011).

8.1.2. Automatic search for a plan based on the application of heuristic rules

This approach relies on a set of **pre-defined rules** that will be applied by a **dedicated planning tool** to generate a suitable expansion plan. There is no a priori guarantee on the goodness of the final solution or on the validity of the rules applied.

The relatively simpler layout of this tools when compared to optimization allows solving **long and medium term expansion planning of systems of all sizes** with a **higher level of modelling detail**. Ideally, the most relevant technical constraints would be considered within the model. Only in the cases where a full system description cannot be achieved, a subsequent feasibility assessment should be carried out.

The most important disadvantage of these methods is that, given the size and complexity of the problem, **the proposed plan may be far from optimal**.

Some applications apply general local search methods that are not specific to the TEP problem. For instance, **GRASP** (Greedy Randomized Adaptive Search Procedure) or **Tabu Search** (which avoids already visited directions by adding them to a restricted or *tabu* list) have been used in applications such as (S. Binato, de Oliveira, & de Araujo, 2001) and (E. L. Da Silva, Ortiz, De Oliveira, & Binato, 2001) respectively.

The application of rules explicitly developed for the TEP problem has also been widespread. Particularly, greedy local search processes guided by **sensitivity analyses** have been very popular (Bennon, Juves, & Meliopoulos, 1982; Cagigas & Madrigal, 2003; Dahman, Morrow, Tynes, & Weber, 2008; Dechamps &

Jamoulle, 1980; Ekwue & Cory, 1984; Escobar , 2002; Latorre-Bayona & Perez-Arriaga, 1994; Levi & Calovic, 1991; Serna, Duran, & Camargo, 1978; Zhao Xu, Zhao Yang Dong, & Kit Po Wong, 2006).

If there is not a clear consensus on what expansion rules should be applied, **Expert Systems** can help extract them by generalizing information available from a set of smaller sample systems (Gajbhiye, Naik, Dambhare, & Soman, 2008; Joong-Rin Shin & Young-Moon Park, 1993; Teive, Silva, & Fonseca, 1998). These rules can then be generalized and applied to the system that is being planned.

The application of expansion rules can easily result in solutions that are far from optimal, as they reflect the necessary limited expertise of the planner and their generalization power is usually limited. Expert systems generalize the behavior of smaller systems and, therefore, may miss effects and structures that arise in larger systems only. Notably, although suitable reinforcements might be adequately detected, it is possible that large *supergrid* investments might be missed, resulting in **suboptimal** solutions. This risk increases as the size of the area under study grows.

8.2. Iterative search for a suitable expansion plan

Iterative search approaches rely on the interaction between a planning module and an operation module.

8.2.1. Planning module

The planning module is aimed at identifying specific reinforcements to be made to the network based on information on system operation made available by the operation module, which has computed the system economic dispatch. Then, for each iteration of the search process, the operation module is run first, considering the grid model defined in the previous iteration, and the planning module runs afterwards. Transmission expansion proposals are aimed at maximizing social welfare (or, equivalently, minimizing total cost). Usually, the planner must explicitly intervene in the selection of these proposals selecting those most promising by combining information resulting from the simulation of the system operation with their expert knowledge. An update of the set of expansion proposals to be deployed is computed in each iteration of the search process.

Given the dependence of this algorithm on expert knowledge collected by the planner, this network planning option seems not well suited to long time horizons, where uncertainty about conditions applying is very high, and large systems, since knowledge of the features of the whole system by any entity is limited.

Defining specific network reinforcements requires considering a detailed model of the system grid and network constraints. Depending on the level of detail of the representation of the network considered in the operating module, two options exist for the analyses to be undertaken within the planning module:

1. The operation module computes the economic system dispatch subject to all relevant network constraints and therefore makes use of a detailed network model. In this case, computing the operation of the system within the planning module may only be necessary to assess the impact on the system dispatch of new transmission lines, i.e. those network investments that do not correspond to the reinforcement (increase in capacity) of an already existing network asset. Assessing the convenience of including such network investments within the network expansion plan may be deemed to require performing sensitivity analyses of system operation with respect to these additions.
2. The operation module makes use of a simplified network model when producing information to be used by the planning module to determine specific network reinforcements. In this case, analyses within the planning module should include the computation of the economic system dispatch making use of a detailed representation of the system network. The operation module may have computed the economic operation of the system through a long period of time, or for a large set of operation

snapshots, and identifies which of these snapshots are to be considered with a higher level of detail in the Planning (network) module. Note that this is the approach adopted by ENTSO-e for the computation of the 2012 TYNDP, see [70].

8.2.2. Operation module

The operation module evaluates the performance of the system considering the network architecture resulting from the reinforcements so far proposed by the planning module. Network performance is assessed according to an agreed set of criteria. The economic dispatch subject to at least the most relevant technical constraints should be incorporated to this calculation.

Given that the planning module may not compute the operation of the system once proposed reinforcements are in place, or this module may not consider all possible operation situations, the reinforcement plan proposed may not be technically feasible. If the proposed network expansion plan generates any technical infeasibility at the operation stage, they are tackled depending on their importance. Small and easily solved infeasibilities are corrected by means of minor modifications to the expansion plan. More important problems are reformulated as constraints for the planning module to take into account in subsequent iterations. The assessment of the technical feasibility of the network architecture considered at each step of the search for the expansion plan may be conducted together with the computation of the economic dispatch or as a subsequent step through the use of a detailed load flow tool.

8.2.3. Analysis of iterative search algorithms

The most fundamental advantage of this technique is its relative **simplicity** and ease of use. Depending on the approach adopted, the planning module can be as straightforward as a communication tool that structures the interaction between the planner and the operation module. In turn, the operation module can be built from any suitable power flow analysis tool.

Network reinforcements proposed at each iteration, and therefore the network architecture finally obtained, is dependent not only on the planner's expertise but also on the particular planning process and cannot be determined exclusively in objective terms. In addition, as explained in the case of automatic heuristic search, although small reinforcements might be appropriately inferred from the data provided by the operation module, other larger investments might be missed if not deliberately proposed by the planner. This can result in solutions that are far from optimal. For this reason, this method is better suited **for medium (not long) term planning of not very large systems** where identifying all potentially relevant network reinforcements making use of expert knowledge and a predetermined set of simple rules may be feasible**.**

Implementations of iterative search approaches can be found in references such as (Lu, Dong, & Saha, 2005; Risheng Fang & Hill, 2003).

8.3. Other considerations

The selected planning approach must be able to include the features that have been deemed necessary for the particular TEP development. This section presents two of the most relevant of these decisions.

8.3.1. Transmission technologies

Different transmission technologies are available for the deployment of new corridors and, as such, should be included in the analysis. Several strategies are possible.

Reinforcements of a corridor using different transmission technologies may be considered as **different candidate network investments**, so that the solution method is left to select not only the optimal grid architecture but also the preferred technological option for its deployment. This has the advantage of not restricting the optimal solution but can greatly increase problem size and burden its resolution.

Alternatively, the most suitable technological option for each corridor can be defined ex-ante following some **heuristic rules**, or ex-post, once the basic network topology has been defined. The latter case implies the definition of a “base case” technology which characteristics are used to define the expansion plan. Once the new corridors have been defined, the decision on the final technological option can be made by means of heuristic rules or a sensitivity analysis that studies the impact of each available choice.

8.3.2. Uncertainty and time structure

Uncertainty appears in the TEP problem at different levels.

At a **long term (scenario) level**, the development of demand, new generation, available technologies and the future evolution of fuel and carbon prices are unknown. These *non random* uncertainties can be dealt with in two alternative ways:

- The **traditional** approach computes the optimal expansion plan for **each static scenario separately**. Then, the *flexible* network additions that appear in many of these scenarios are selected.
- Alternatively, **enhanced approaches** find plans that are able to dynamically adapt to a multiplicity of scenarios as they develop and its multi-stage nature. Some of the most relevant techniques that have been applied to deal with this dimension of the problem are classical optimization methods (Kaltenbach, Peschon, & Gehrig, 1970; Meliopoulos et al., 1982; Meza et al., 2007; Sharifnia & Aashtiani, 1985; Vinasco et al., 2011; Youssef & Hackam, 1989) and, in particular, dynamic programming (DP) (Dusonchet & El-Abiad, 1973; Vasquez, Styczynski, & Vargas, 2008) , and non-classical optimization methods (Braga & Saraiva, 2005; El-Keib, Jaeseok Choi, & Trungtinh Tran, 2006; Escobar , 2002; Hesamzadeh, Hosseinzadeh, & Wolfs, 2008; Maghouli, Hosseini, Buygi, & Shahidehpour, 2011; Miranda & Proenca, 1998a; Miranda & Proenca, 1998b; Rezende, Leite da Silva, & Honorio, 2009; Romero, Rider, & Silva, 2007; Sum-Im, Taylor, Irving, & Song, 2009; Xie, Zhong, & Wu, 2007).

In the **short term**, several snapshots that are representative of the whole horizon year are included in the system operation calculation. The background scenario is considered as given, and the remaining relevant snapshots can be selected from the market analysis performed in task 2.3. If necessary, clustering techniques can be applied in order to reduce the size of the scenario tree (J. M. Latorre, Cerisola, & Ramos, 2007).

8.4. Conclusions

Several methodologies are available for network expansion planning. Their main features as well as their most important advantages and potential drawbacks are summarized in the following list.

Automatic techniques have, once the problem has been defined, no need for further human intervention. Two main approaches can be distinguished:

- **Optimization** methods find the best solutions in terms of the agreed criteria
- **Automatic search** applies a set of heuristic rules to the system

Automatic approaches:

- Are able to deal with medium to long term planning of systems of all sizes
- Can cope with a level of modeling detail that depends on the computation burden of the specific solution method used. Thus, classical optimization requires a simpler representation of the system functioning than automatic search.
- Are objective
- In particular, classical optimization:
    - Can guarantee the optimality of the expansion plan
    - Given the need to consider a relatively simple description of system operation, a subsequent feasibility assessment of the solution needs to be carried out
- Heuristic searches:
    - In general are able to accommodate a higher level of detail compared to classical optimization
    - Are at risk of arriving to suboptimal solutions

These methods are able to compute the long term expansion of the grid of large systems, where uncertainty on the set of conditions existing in the relevant time frame is high and the set of potential reinforcements of different types to be considered is very large.

Iterative search techniques seek for a suitable expansion plan that is unlikely to be the truly optimal solution by combining information from two different modules:

- A planning module proposes new investments at each iteration of the process taking into account available system information.
- An operation module updates system information having into account the proposed investments.

As explained earlier, these methods:

- Are suitable for medium term planning of not very large systems (not very well suited to the large term expansion planning of the EU system)
- Are relatively easy to implement.
- Fully depend on the planner's expertise and the specific decision process.
- Present a relatively high risk of arriving to suboptimal solutions.

9. Appendix B: DC approximation

In this section, the derivation of the active and reactive power flow equations of any transmission line are detailed in first part. Then, the DC approximation is presented, starting from these equations.

Power flow equations

Figure 21 gives the common π representation of a transmission line ik $(i \neq k)$, using complex notations (where $j = \sqrt{-1}$).

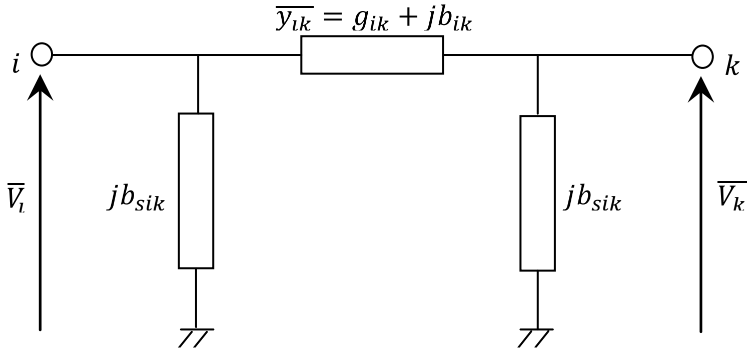

Figure 21. Schematic representation of a transmission line $\boldsymbol{ik}$

The branch impedance can be written as $\overline{z_{ik}} = r_{ik} + jx_{ik}$, where r_{ik} is the branch resistance and x_{ik} is the branch reactance, and the branch admittance is expressed as $\overline{y_{ik}} = g_{ik} + jb_{ik}$, where g_{ik} is the branch conductance and b_{ik} is the branch susceptance.

As the admittance is the inverse of the impedance, the following relations are derived:

$$\overline{y_{ik}} = \frac{1}{\overline{z_{ik}}} = \frac{1}{r_{ik} + jx_{ik}} = \frac{(r_{ik} - jx_{ik})}{(r_{ik} + jx_{ik})(r_{ik} - jx_{ik})} = \frac{r_{ik}}{r_{ik}^2 + x_{ik}^2} + j\,\frac{-x_{ik}}{r_{ik}^2 + x_{ik}^2}$$

$$\Rightarrow \begin{cases} g_{ik} = \dfrac{r_{ik}}{r_{ik}^2 + x_{ik}^2} \\ b_{ik} = \dfrac{-x_{ik}}{r_{ik}^2 + x_{ik}^2} \end{cases}$$

Let $\overline{S_{ik}}$ be the complex power flow of branch ik, P_{ik} the real branch power flow and Q_{ik} the reactive branch power flow. The mathematical relationship among them can be expressed using complex numbers:

$$\overline{S_{ik}} = P_{ik} + jQ_{ik}$$

Where

$$\overline{S_{ik}} = \overline{V_i}\,\overline{I_{ik}}^{*}$$[1]

$$\overline{V_i} = V_i \cos\theta_i + jV_i \sin\theta_i$$

According to Ohm's law, the complex current can be expressed as follows:

[1] The notation $\overline{X}^{\,*}$ refers to the complex conjugate of $\overline{X}$.

$$\overline{I_{ik}} = \frac{\overline{V_i} - \overline{V_k}}{\overline{Z_{ik}}} = \frac{\overline{V_i} - \overline{V_k}}{r_{ik} + jx_{ik}}$$

Thus:

$$\overline{S_{ik}} = \overline{V_i}\frac{\overline{V_i}^* - \overline{V_k}^*}{\overline{Z_{ik}}^*}$$

$$\overline{S_{ik}} = [V_i \cos\theta_i + jV_i \sin\theta_i]\frac{[V_i \cos\theta_i - jV_i \sin\theta_i] - [V_k \cos\theta_k - jV_k \sin\theta_k]}{r_{ik} - jx_{ik}}$$

$$\overline{S_{ik}} = \frac{[V_i^2\cos^2\theta_i + V_i^2\sin^2\theta_i] - V_i[\cos\theta_i + j\sin\theta_i]\, V_k[\cos\theta_k - j\sin\theta_k]}{r_{ik} - jx_{ik}}$$

$$\overline{S_{ik}} = \frac{V_i^2 - V_iV_k[(\cos\theta_i\cos\theta_k + \sin\theta_i\sin\theta_k) + j(\sin\theta_i\cos\theta_k - \cos\theta_i\sin\theta_k)]}{r_{ik} - jx_{ik}}$$

$$\overline{S_{ik}} = \frac{(r_{ik} + jx_{ik})\cdot(V_i^2 - V_iV_k[\cos(\theta_i - \theta_k) + j\sin(\theta_i - \theta_k)])}{(r_{ik} + jx_{ik})\cdot(r_{ik} - jx_{ik})}$$

$$\overline{S_{ik}} = \frac{r_{ik}V_i^2 - V_iV_k[r_{ik}\cos(\theta_i - \theta_k) - x_{ik}\sin(\theta_i - \theta_k)]}{r_{ik}^2 + x_{ik}^2} + j\frac{x_{ik}V_i^2 - V_iV_k[r_{ik}\sin(\theta_i - \theta_k) + x_{ik}\cos(\theta_i - \theta_k)]}{r_{ik}^2 + x_{ik}^2}$$

$$\overline{S_{ik}} = \left(V_i^2 g_{ik} - V_iV_k[g_{ik}\cos(\theta_i - \theta_k) + b_{ik}\sin(\theta_i - \theta_k)]\right) + j(-V_i^2 b_{ik} - V_iV_k[g_{ik}\sin(\theta_i - \theta_k) - b_{ik}\cos(\theta_i - \theta_k)]) = P_{ik} + jQ_{ik}$$

Finally, we obtain the branch real and reactive power equations:

$$P_{ik} = V_i^2 g_{ik} - V_iV_k[g_{ik}\cos(\theta_i - \theta_k) + b_{ik}\sin(\theta_i - \theta_k)]$$

$$Q_{ik} = -V_i^2 b_{ik} - V_iV_k[g_{ik}\sin(\theta_i - \theta_k) - b_{ik}\cos(\theta_i - \theta_k)]$$

DC approximation

Non linear AC Optimal Power Flow (OPF) problems are commonly approximated by more tractable linearised DC OPF problems focusing on real power, especially for large power networks. Non linear constraints, such as balance, branch flow and production for real and reactive power, are linearized using the DC approximation. The following assumptions are made:

(1) The voltage magnitude is supposed uniform at each node. Consequently, the variables are normalised and expressed in *per unit* (pu) values.

(2) The resistance for each branch is negligible compared to the reactance ($r \ll x$).

(3) The voltage angle difference $\theta_i - \theta_k$ across any branch is small enough so that cos $(\theta_i - \theta_k)$ and sin $(\theta_i - \theta_k)$ can be linearised.

Let i and k be two nodes ($i \neq k$) connected by the branch ik. Let P_{ij} be the real power flow and Q_{ik} the reactive power flow of branch ik. Finally, let V_i and θ_i(resp. V_k and θ_k) be the voltage magnitude and voltage angle at node i (resp. k), and let g_{ik} and b_{ik} be the conductance and the susceptance for branch ik.[2]

Using Ohm's law, the real and reactive power flows can be expressed as follows (such as presented above):

$$P_{ik} = V_i^2 g_{ik} - V_i V_k [g_{ik} \cos(\theta_i - \theta_k) + b_{ik} \sin(\theta_i - \theta_k)]$$
$$Q_{ik} = -V_i^2 b_{ik} - V_i V_k [g_{ik} \sin(\theta_i - \theta_k) - b_{ik} \cos(\theta_i - \theta_k)]$$

Given the DC approximation assumptions, the following simplifications are made:

(1) $V_i = V_k = V_0$
(2) $g_{ik} = 0$
(3) $\cos(\theta_i - \theta_k) \approx 1$ and $\sin(\theta_i - \theta_k) \approx \theta_i - \theta_k$

Thus, both real and reactive power flow equations can be linearised as follows:

$$P_{ik} = -V_0^2 \cdot b_{ik} \cdot (\theta_i - \theta_k)$$
$$Q_{ik} = -V_0^2 \cdot b_{ik} - V_0^2 \cdot b_{ik} \cdot 1 = 0$$

Let B_{ik} be the negative branch susceptance (i.e. $B_{ik} = \frac{x_{ik}}{r_{ik}^2 + x_{ik}^2}$) and the voltage magnitude normalised to 1 pu, the real power flow on branch ik can be expressed in this simple form:

$$F_{ik} = B_{ik} \cdot (\theta_i - \theta_k)$$

[2] The impedance of a branch is defined as $z = r + jx$, where r is the resistance (in ohms) and x is the reactance (in ohms). The admittance is defined as the inverse of the impedance, and can be written as $y = g + jb$, where g is the conductance given by $g = \frac{r}{r^2 + x^2}$ (in mhos) and b is the susceptance given by $b = \frac{-x}{r^2 + x^2}$ (in mhos).

10. Appendix C: Adjustment costs

Priority order: upward changes

Upward changes consist in increasing generation or decreasing consumption. The typical priority order for a situation where there is not enough power in the system is illustrated in Figure 22.

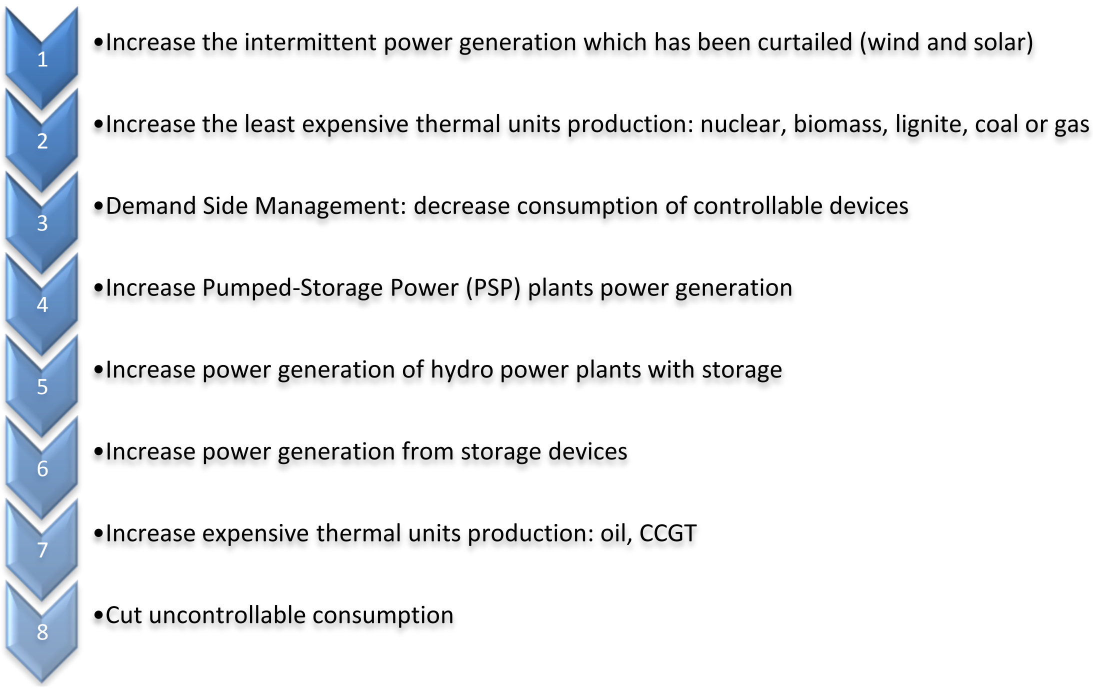

Figure 22. Priority order for upward changes

In the adequacy simulation model in copperplate, all available thermal units with the lowest marginal costs run at their maximum capacity. Thus, the flexibility of thermal units is very low, as most of the operating units are already at their maximum production level. Consequently, most upward changes may be done on hydro generation.

Priority order: downward changes

Downward changes correspond to a situation where there is too much power in the system. Generation has to be curtailed or controllable consumption should be increased according to a particular priority order, defined in Figure 23.

1 •Decrease expensive thermal units production: oil, CCGT

2 •Increase pumping (i.e. power consumption) of Pumped-Storage Power (PSP) plants

3 •Increase energy storage in storage devices

4 •Demand Side Management: increase consumption of controllable devices

5 •Decrease less expensive thermal units production: nuclear, biomass, lignite, coal and gas

6 •Decrease power generation of hydro plants with storage

7 •Curtail intermittent wind and solar generation

8 •Shut-down operating thermal units

Figure 23. Priority order for downward changes

Definition of adjustment costs

Then, starting from these priority orders, we defined adjustment costs for each injection type (Table VIII, the list of injection types is not exhaustive). These values were defined for the purpose of testing the methodology. Sensitivity analyses would be necessary for a validation process, but we did not have time to perform them.

Table VIII - Definition of adjustment costs

Injection type	c^+ *(Increase generation or decrease consumption)*	c^- *(Decrease generation or increase consumption)*
Wind/Solar	Cannot be modified, except in the case of curtailment (zero cost)	2ϵ[3]
Thermal	MAX (System cost, Generation cost)	- Generation cost + ϵ
Hydro Run-Of-River	Cannot be modified	Cannot be modified
Hydro with storage	Stored energy cost + 2ϵ	ϵ
Hydro PSP	Stored energy cost + ϵ	- Stored energy cost + 2ϵ
Centralised storage	Stored energy cost + 3ϵ	- Stored energy cost + 3ϵ
Demand-side management	Stored energy cost + 4ϵ	- Stored energy cost + 4ϵ
Unsupplied energy	Cost of unsupplied energy (10000€/MWh)	

The system cost is the cost of the most expensive operating thermal unit. It is calculated in the adequacy simulations and corresponds to the dual variable of the balance constraint (generation = consumption).

The stored energy cost is the value of 1MWh of stored energy optimally used over a week. It is equal to the dual variable of the balance constraint which links the energy pumped and the energy generated during one week. This is an output from the adequacy simulations.

[3] ϵ is a negligible positive cost (e.g. 0.1€/MWh) used to classify the different injection types